Am J Cancer Res 2024;14(3):1316-1337
www.ajcr.us /ISSN:2156-6976/ajcr0153915

Original Article

Integrated analysis of lactate-related genes identifies POLRMT as a novel marker promoting the proliferation, migration and energy metabolism of hepatocellular carcinoma via Wnt/β-Catenin signaling

Huifen Wang, Yanli Zhang, Shiyu Du

Department of Gastroenterology, China-Japan Friendship Hospital, Beijing 100029, P. R. China

Received October 14, 2023; Accepted March 13, 2024; Epub March 15, 2024; Published March 30, 2024

Abstract: Hepatocellular carcinoma (HCC) is a prevalent and deadly form of cancer globally with typically unfavorable outcomes. Increasing research suggests that lactate serves as an important carbon contributor to cellular metabolism and holds a crucial part in the progression, sustenance, and treatment response of tumors. However, the contribution of lactate-related genes (LRGs) in HCC is still unclear. In this study, we analyzed TCGA datasets and screened 21 differentially expressed LRGs related to long-term survivals in HCC patients. Pan-cancer assays revealed that 21 LRGs expression exhibited a dysregulated level in man types of tumors and associated with clinical prognosis of tumor patients. The analysis of 21 LRGs successfully classified HCC samples into two molecular subtypes, and these two subtypes showed significant differences in clinical information, gene expression, and immune characteristics. Subsequently, based on the aforementioned 21 LRGs, a novel prognostic signature (DTYMK, IRAK1, POLRMT, MPV17, UQCRH, PDSS1, SLC16A3, SPP1 and LDHD) was generated by LASSO-Cox regression analysis. Survival assays demonstrated that the signature performed well in predicting the overall survival of patients with HCC. The results of Gene Set Variation Analysis indicated that the high GSVA scores were associated with poor prognosis. Moreover, we also investigated the correlation between GSVA scores and various signaling pathways in HCC. Among the nine prognostic genes, our attention focused on POLRMT which was highly expressed in HCC specimens based on TCGA datasets and several HCC cell lines. In addition, functional assays indicated that POLRMT distinctly promoted the proliferation, migration and energy metabolism of HCC cells via regulating Wnt/β-Catenin signaling. Overall, through the establishment of a novel prognostic signature, we have provided potential clinical value for assessing the prognosis of HCC patients. Furthermore, our study has identified the high expression of POLRMT in HCC and demonstrated its crucial role in HCC cell proliferation. These findings hold great importance in advancing our understanding of the pathophysiology of HCC, identifying new therapeutic targets, and improving patient survival rates.

Keywords: Hepatocellular carcinoma, lactate, biomarker, prognostic signature, tumor microenvironment, POLRMT, Wnt/β-Catenin signaling

Introduction

Hepatocellular carcinoma (HCC) represents a type of malignant tumor that ranks sixth in global cancer diagnoses and is the fourth primary reason for cancer-associated fatalities worldwide [1]. HCC has a significantly varying incidence rate across different regions globally. Asian countries, particularly East Asia and Southeast Asia, are high-incidence areas for HCC. China, Japan, South Korea, Vietnam, and Taiwan are some of the regions where the reported liver cancer rates are higher [2]. Additionally, sub-Saharan Africa is also considered a high-risk region for liver cancer. Chronic hepatitis B virus and hepatitis C virus infections, alcoholism, diabetes, and the metabolic syndrome are all known to increase the likelihood of developing HCC [3]. Despite numerous improvements in HCC detection because of advances in treatment, pateints with HCC still have a dismal chance of survival due to the disease's high metastatic rate [4, 5]. In addition, the prognosis of HCC patients is significantly

https://doi.org/10.62347/ZTTG4319

impacted by the fact that over 70% of patients who have surgical resection or ablation experience tumor recurrence within 5 years [6, 7]. Given the significant burden of HCC on a global scale, there is an urgent need to explore novel prognostic markers that can aid in early detection, accurate prognosis, and personalized treatment strategies. Identifying reliable prognostic markers for HCC could revolutionize clinical practice, allowing healthcare professionals to offer timely and targeted interventions, thereby improving patient outcomes and survival rates.

High-throughput sequencing, also known as second-generation or deep sequencing, is a rapid and efficient DNA or RNA sequencing technology [8]. It is a method used for large-scale, high-throughput determination of sequences in genomes, transcriptomes, or other biological molecules. The development of high-throughput sequencing technology allows researchers to obtain a vast amount of DNA or RNA sequence information in a relatively short time and at lower costs [9, 10]. High-throughput sequencing technology can help scientists gain a deep understanding of genetic variations and mutations in tumor cells, including single nucleotide variants (SNVs), insertions and deletions (InDels), chromosomal structural variations, and more. This information is crucial for understanding the mechanisms underlying tumor development, identifying key genes driving cancer progression, and identifying potential therapeutic targets [11]. By performing RNA sequencing on tumor samples, researchers can reveal which genes in tumor cells are actively expressed, which genes' expression is regulated, and the functional state of the cells. This is highly beneficial for discovering novel gene expression patterns related to cancer, understanding the heterogeneity of tumor cells, and predicting patient prognosis. Epigenetics refers to the regulation of gene expression through non-sequence changes, such as DNA methylation and histone modifications [12, 13]. High-throughput sequencing technology can assist researchers in understanding these epigenetic alterations in tumor cells, thereby gaining insight into the regulatory mechanisms and identifying epigenetic markers associated with cancer. Overall, high-throughput sequencing technology provides comprehensive and efficient information in cancer research, including genomics, transcriptomics, epigenetics, and more. It offers robust support for unraveling the mechanisms of tumorigenesis, cancer classification, the development of treatment strategies, and personalized medicine.

Lactate was long regarded as an end product of cellular glycolysis. In living organisms, lactic acid is an essential metabolite. It can be produced and metabolized through two pathways: lactic acid fermentation (lactic acid production) or lactic dehydrogenase (LDH)-mediated lactic acid dehydrogenation (lactic acid consumption) [14]. Lactic acid metabolism refers to the production and consumption of lactic acid in the body. In lactic acid fermentation, when there is a lack of oxygen or inadequate oxygen supply, cells cannot produce enough energy through normal oxidative phosphorylation (aerobic metabolism) [15]. As a result, they switch to producing lactate as a metabolic byproduct. Lactic dehydrogenase is an enzyme that, under sufficient oxygen conditions, converts lactic acid back into pyruvic acid to continue aerobic metabolism [16, 17]. Lactic acid metabolism is closely related to the occurrence and development of tumors. In tumor tissues, rapidly proliferating cancer cells require a large amount of energy and nutrients to support their growth and division. Often, the oxygen supply in tumors is insufficient, leading to local hypoxia. This prompts tumor cells to produce lactic acid through lactic acid fermentation to sustain their survival and proliferation [18, 19]. This phenomenon is known as "acidosis", wherein lactic acid accumulation in tumor tissues lowers the pH value. Lactate also plays other significant roles in tumor development. It can function as a signaling molecule, regulating the migration and invasion capabilities of tumor cells and promoting tumor metastasis and spread. Additionally, lactic acid can influence the tumor microenvironment, suppressing the function of immune cells, thereby aiding tumors in evading immune attacks and creating immune escape. The important roles of lactate metabolism highlighted the potential of lactate-related genes used as novel prognostic biomarkers and therapeutic targets for HCC patients.

In this study, we systematically analyzed the identified LRGs in HCC patients using TCGA and ICGC datasets. Then, the prognosis of HCC patients was evaluated using a lactate-related

prognostic signature (LRPS) comprised of nine genes. We also investigated how the LRPS relates to other aspects of the immunological microenvironment. Finally, our attention focused on POLRMT and performed a series of experiments to further explore the function of POLRMT in HCC. Our study has provided a comprehensive understanding of the relationship between lactic acid metabolism and HCC, offering valuable insights for patient prognosis assessment and guidance in immunotherapy. Additionally, we have revealed the potential functions and mechanisms of POLRMT in HCC, which is of significant importance for a deeper comprehension of HCC pathogenesis and the exploration of novel therapeutic approaches. Our research findings open up new avenues and possibilities for future clinical treatments and personalized medicine in HCC.

Materials and methods

Cell lines and cell transfection

Human liver cancer cell lines HepG2, Hep3B, SNU-423, SNU-387 cells, were obtained from the China Center for Type Culture Collection (Wuhan, Hubei, China), and other liver cancer cell lines including JHH-2, Huh-7, SMMC-7721, SNU-449 cells, and normal liver cell line LO2, were purchased from Wuhan Procell company (Wuhan, Hubei, China). JHH-2 and SNU-449 cells were purchased from Cobioer company (Nanjing, Jingsu, China). The cells were cultured in RPMI-1640 media supplemented with 10% heat-inactivated FBS (Excell, Taicang, Jiangsu, China), and grown in the presence of penicillin/streptomycin (Qianye Biotechnology, Changsha, Hunan, China) in a 37°C incubator with a humidified, 5% CO_2 atmosphere.

Cell transfection

The POLRMT siRNA sequence (siRNA-POLRMT-1: GGAGCUGGUAUAUGUGUUA, siRNA-POLRMT-2: GAGAUGCUGGUGCAGGCUA), and negative control siRNA sequence (CGUACGCGGAAUACUUCGAUU) obtained from GenePharma (Pudong, Shanghai, China). The POLRMT overexpressing plasmids were constructed by Generay Technologies (Pudong, Shanghai, China). The transfection of POLRMT siRNAs or overexpressing plasmids were performed using Lipofectamine 3000 reagent kits (ThermoFisher, Pudong, Shanghai, China). According to the manufacturer's instructions, siRNAs being diluted in the 100 μl Opti-MEM (Invitrogen, Carlsbad, CA, United States) at 5 nmol/L or 5 μg plasmids were mixed with 5 μL Lipofectamine 3000 reagents. After incubation at room temperature for 20 min, the mixtures were added to the cell culture media, and the cells were collected or used for experiments after 48-72 h.

CCK-8 assays

CCK-8 assays were utilized for the determination of HCC cells growth abilities, and performed by using CCK-8 kits from Beyotime company (Nantong, Jiangsu, China). Briefly, HCC cells including Huh7 and Hep3B in log phase growth were trypsinized with a 0.05% trypsin solution, washed, and planted in 96-well plates at a concentration of 2.5×10^3 cells/well. After the HCC cells attachment, 10 μL of the CCK-8 solution was added into each well and continue to culture for another 3 hours at 37°C. Thereafter, the optical density value at 450 nm was recorded at the indicated time point (24, 48 and 72 h).

The 5-ethynyl-2'-deoxyuridine (EDU) incorporation assays

For the EDU incorporation assays, HCC cells transfected with siRNA-POLRMT-1, siRNA-POLRMT-2 or pcDNA3.1-POLRMT, were cultured in 24-well plates, and then the Click-iT EDU Alexa Fluor 488 Imaging Kits (ThermoFisher, Pudong, Shanghai, China) were used to carry out the experiments. Briefly, the HCC cells were incubated with EdU (10 μM) and fixed with 4% paraformaldehyde (PFA; Sigma, Pudong, Shanghai, China), followed by treatment with Triton X-100 solution. Thereafter, the cells were stained with the 1 × Apollo reaction cocktail and the nuclei were stained by DAPI reagents. After washing with PBS for three times, the fluorescence of the cells was visualized by using an Olympus fluorescence microscope (Tokyo, Japan).

Transwell migration detection

The migration capabilities of Huh7 and Hep3B cells after being transfected with siRNA-POLRMT-1, siRNA-POLRMT-2 or pcDNA3.1-POLRMT, were evaluated by using transwell chambers (Corning, NY, USA). In brief, a total of 2×10^3 cells with treatment in 200 μl serum-free media were placed in the upper chamber of 24-well

plates with 8.0 μm pore size chamber inserts. Afterwards, 700 μl RPMI-1640 media contained 10% FBS were added to the lower chambers. Cells were fixed with 4% paraformaldehyde and stained with 0.1% crystal violet solution after being incubated at 37°C for 24 hours. The red-stained cells were seen under an inverted microscope after being washed twice with PBS.

Real-time PCR detection

The mRNA levels of POLRMT in HCC cell lines, and Huh7 and Hep3B cells after being transfected with siRNA-POLRMT-1, siRNA-POLRMT-2 or pcDNA3.1-POLRMT, were determined by qRT-PCR assays using the PerfectStart Green qRT-PCR SuperMix Kits (TransGen Biotech, Beijing, China). The total RNAs were extracted by Trizol reagents (ThermoFisher, Pudong, Shanghai, China) and the cDNAs were synthesized using the PrimeScript® RT Reagent Kit (Takara, Dalian, Liaoning, China). Thereafter, the real-time PCR were then carried out using the above mentioned supermix kits, and the reaction conditions were as following: 95°C for 10 s and 60°C for 60 s, repeating for 40 cycles. The relative expression of POLRMT was calculated by $2^{-\Delta\Delta Ct}$ methods. GAPDH was measured as an internal control. The primers were obtained from Generay Technologies (Pudong, Shanghai, China), and the primer sequences were as following: 5'-CCACATCGCTCAGACACCAT-3' (sense) and 5'-ACCAGGCGCCCAATACG-3' (antisense) for GAPDH, and 5'-GGACTCCCCGGCAAAGAAG-3' (sense) and 5'-CGCCACATCCACCCTGTTC-3' (antisense) for POLRMT.

Western blot determination

Briefly, Huh7 and Hep3B cells after being transfected with siRNA-POLRMT-1, siRNA-POLRMT-2 or pcDNA3.1-POLRMT, were collected and they were lysed using RIPA buffer reagent kits (ThermoFisher, Pudong, Shanghai, China) at 4°C for 15-20 min, followed by centrifugation at 10000 rpm for 10 min at 4°C. The supernatants were collected and mixed with 4 × sample loading buffer (Life Technologies, Pudong, Shanghai, China). Then, the lysates were subjected to 8-12% SDS-PAGE gels. After the proteins were transfered onto the PVDF membranes (Millipore, Darmstadt, Germany), the blots were blocked in TBST and 5% BSA for 1 h at room temperature. Afterwards, the blots were separately incubated with primary antibodies against β-Catenin (1:1000; Abcam, Pudong, Shanghai, China), cyclin D1 (1:1500; Abcam, Pudong, Shanghai, China), c-Myc (1:1200; ProteinTech, Wuhan, Hubei, China), and β-actin (1:12000; ProteinTech, Wuhan, Hubei, China), for 12 h at 4°C. Blots were then washed thrice with TBST and incubated with corresponding secondary antibodies for 1 h. Then, the blots were incubated with ECL kits (Madison, WI, USA) and exposed in ChemiDox XRS (Bio-Rad, Hercules, CA, USA).

ATP contents detection

The ATP contents was measured using Beyotime Biotechnology's ATP content detection kits (Nantong, Jiangsu, China). Briefly, the Huh7 and Hep3B cells after being transfected with siRNA-POLRMT-1, siRNA-POLRMT-2, were respectively placed in six-well plates, followed by being lysed with lysate buffer solution (Beyotime Biotechnology, Nantong, Jiangsu, China). The lysates were collected and centrifuged at 12,000 g for 5 min at 4°C. Then, the total protein concentration of each sample was quantified using BCA assay kits (Beyotime Biotechnology, Nantong, Jiangsu, China). After that, the samples of each groups were added into ATP measurement solution, and the ATP contents were determined by using a fluorescence microplate reader. The relative ATP contents were standardized by the total protein contents.

Data collection and the screening of differentially expressed genes (DEGs)

The gene expression data and clinical information from tumor and normal tissues of liver hepatocellular carcinoma (LIHC) were downloaded from TCGA datasets. The 335 lactate related genes (LRG) were selected from MSigDB database (https://www.gsea-msigdb.org/gsea/index.jsp). The genes which were significantly correlated with overall survivals in HCC based on TCGA data (UALCAN-OS) were collected from UALCAN database (https://ualcan.path.uab.edu/index.html). The deferentially expressed genes (DEGs) in HCC based on TCGA data were analyzed by using R software "limma" package, and P-value < 0.05 and $|\log2(FC)| > 1$ were defined as the threshold of DEGs. The overlap DEGs among TCGA-DEGs, LRG and UALCAN-OS were obtained by using

Venny2.1 (https://bioinfogp.cnb.csic.es/tools/venny/). The heatmap and volcano map in the presented study were generated by using R package "ggplot".

Gene functional enrichment and gene correlation analysis

Gene Ontology (GO) and Kyoto Encyclopedia of Genes and Genomes (KEGG) analysis were carried out using R software package "clusterProfiler". For multi-gene correlation analysis, the gene expression data in HCC were downloaded from TCGA database (different HCC grades, TCGA-LIHC) and International Cancer Genome Consortium (ICGC) database (https://icgc.org/). The multi-gene correlation heatmap was displayed by the R software package "ggstatsplot".

The immune infiltration analysis

Two algorithms, including CIBERSORT and XCELL, were applied for the analysis of immune infiltration in HCC through R software based on TCGA data. To assess the immune score, we used R software package "immuneeconv", and the immune checkpoint genes expression in different groups were visualized by R software package "ggplot2". The immune networks of common DEGs or POLRMT with kinds of immune cells were analyzed by R software package "immuneeconv" and constructed by using R software package "ggClusterNet". The tumor mutation burden (TMB) and microsatellite instability (MSI) analysis of POLRMT in pan-cancers were also carried out by using R software.

Online websites for bioinformatics analyses

The DEGs or POLRMT expression, various survivals, genetic changes (SNV and CNV) across pan-cancers or in HCC, were analyzed by using the Gene Set Cancer Analysis (GSCA) database (http://bioinfo.life.hust.edu.cn/GSCA/#/) or TIMER 2.0 database (http://timer.cistrome.org/). The Human protein atlas (HPA, https://www.proteinatlas.org/) was utilized for analyzing the POLRMT protein expression in pan-cancers and its immunohistochemistry in HCC tumor tissues. GeneMania (https://GeneMANIA) database to analyze genes or proteins which were able to interact or co-express with POLRMT. The CCLE database (https://portals.broadinstitute.org/ccle) was queried for transcriptome information from HCC cell lines. GEPIA database (http://gepia.cancer-pku.cn/) was utilized for analyzing gene expression and survivals.

Statistical analysis

Statistical analysis was performed using SPSS16.0 statistical software (SPSS, Chicago) and R version 3.5.2. Values were expressed as mean ± SEM. Multiple group comparisons were made using one-way analysis of variance. To determine statistical significance, we applied a cutoff of $P < 0.05$.

Results

Verifying overlap DEGs in HCC and functional enrichment analysis

To discover the potential therapeutic target of HCC based on 335 lactate-related genes (LRGs), we first employed R software to obtain the aberrantly differentially expressed genes (DEGs) in HCC tumor tissues compared with HCC adjacent normal tissue samples. The DEGs were consisted with 2451 up-regulated genes and 446 down-regulated genes. Then, the genes with significant overall survival (OS) in TCGA-LIHC were obtained by using UALCAN database (https://ualcan.path.uab.edu/index.html), and there were 5759 genes. Consequently, we certified 20 overlap genes of TCGA-up-DEGs, LRGs and UALCAN-OS, and only 2 overlap genes of TCGA-down-DEGs, LRGs and UALCAN-OS (**Figure 1A**). Afterwards, we performed a univariate Cox regression (uniCox) analysis of these 22 DEGs, and the 21 survival-related DEGs (except AARS2) were retained for further analysis (**Figure 1B**). The 21 DEGs were then subjected to gene functional enrichment analyses including GO analysis and KEGG analysis. The results from GO analyses demonstrated that the 21 DEGs were related with tRNA modification, mitochondrial RNA metabolic process, tRNA metabolic process, D-lactate dehydrogenase (cytochrome) activity, catalytic activity, acting on a tRNA, tRNA binding catalytic activity, acting on RNA, mitochondrial respiratory chain complex III, mitochondrial protein-containing complex, mitochondrial matrix (**Figure 1C-E**). The KEGG analysis revealed that the 21 DEGs were correlated with Terpenoid backbone biosynthesis (**Figure 1F**).

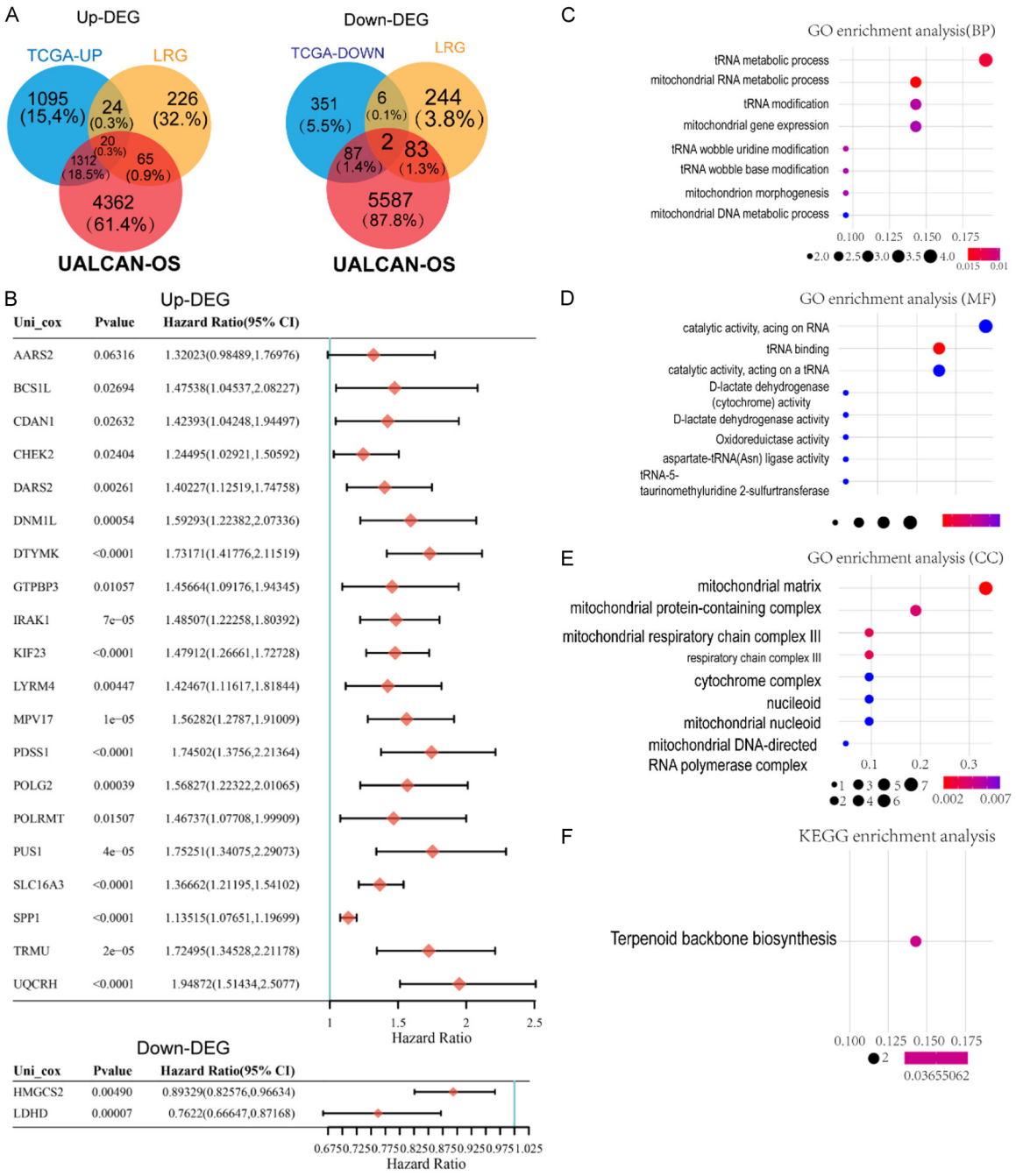

Figure 1. Screening overlap DEGs and functional enrichment analysis. A. Venn diagram of the DEGs, prognostic genes and LRGs. B. Univariate Cox regression (uniCox) analysis. C-E. GO analysis. F. KEGG analysis.

The DEGs' expression, genetic variants, and methylation analyses in pan-cancer

Next, we sought to explore the mRNA expression, genetic changes, and methylation status of the above-selected 21 DEGs across TCGA cancers. By employing GSCA database (http://bioinfo.life.hust.edu.cn/GSCA/#/), the 21 DEGs' mRNA expression was investigated and the bubble plots presented that the most of the 21 DEGs were significant up-regulated in many cancer types including LUSC, LIHC, LUAD, STAD, BRCA, BLCA and COAD (Supplementary Figure 1A). The DEGs' expression in various cancers' stages including clinical stages and pathological stages was also evaluated, and

the data suggested that there were expression differences of these DEGs in clinical stages and pathological stages of many TCGA cancers such as UVM, UCS, UCEC, OV, LIHC, COAD (Supplementary Figure 1B). Subsequently, the single nucleotide variant (SNV) mutation frequency of DEGs was analyzed, and the data revealed that the variant classification of these DEGs was mainly missense mutation, and the top 10 mutated genes were POLRMT, CDAN1, CHEK2, KIF23, HMGCS2, DNM1L, DARS2, IRAK1, GTPBP3, and POLG2 (Supplementary Figure 1C). Moreover, the copy number variation (CNV) mutation frequencies of these DEGs were also explored, and the data from the pie plots displayed that the 21 DEGs had CNV especially heterozygous amplification in most cancers (Supplementary Figure 1D). Besides, the methylation of these DEGs were studied, and we found that most of the DEGs were low methylation in kinds of cancers particularly in KIRC, LUSC, KIRP, BLCA, HNSC and BRCA (Supplementary Figure 1E).

The correlation analyses of DEGs based on TCGA and ICGC databases

The DEGs might exist correlations between each other in HCC tumor tissues. We thereby next attempted to discover the correlation difference of the DEGs in different grades of HCC based on TCGA and ICGC databases. The four grades (grade 1, grade 2, grade 3 and grade 4) of HCC samples from TCGA database respectively had 55, 177, 122 and 12 samples. We then analyzed the correlations of the 21 DEGs in these four grades of HCC, and we found that the down-DEGs (HMGCS2 and LDHD) were negative correlation with other DEGs in all these four HCC grades' samples, while other up-DEGs were all positive correlation with each other (**Figure 2A-D**). Similar results were observed in ICGC-liver cancer-RIKEN sub-database (161 HCC samples) that the up-DEGs were positive related with each other, and the two down-DEGs (HMGCS2 and LDHD) were negative related with other DEGs (**Figure 2E**). However, the results from ICGC-liver cancer-France sub-database (240 HCC samples) were some different. The data displayed that HMGCS2 and LDHD were positively correlated with most up-DEGs, which might imply that the HCC tumor samples had very complex heterogeneity (**Figure 2F**).

Identification of the molecular subtypes of HCC using DEGs

We next wonder whether the 21 DEGs were capable to distinguish the TCGA-LIHC smaples into different molecular subtypes. To achieve that, the R software "ConsensusClusterPlus" package was applied to identify molecular subtypes of 371 HCC samples. After analysis, the consensus cumulative distribution function (CDF) plot, the delta area, the consensus matrix were obtained, and the data suggested that the 371 HCC samples was able to be divided into two molecular subtypes including C1 group (103 HCC samples) and C2 group (268 HCC samples) using the 21 DEGs (**Figure 3A-C**). The heatmap of these two molecular subtypes was presented in **Figure 3D**. In addition, the overall survival difference of these two molecular subtypes was also investigated, and the results proved that C1 group had poor survivals than that of C2 group (**Figure 3E**).

Clarification of the deferentially expressed genes in the two HCC molecular subtypes

Since our above data had revealed that the 21 DEGs could divided 371 TCGA-LIHC samples into two subgroups (C1 group included 103 HCC samples and C2 included 268 HCC samples), we next sought to verify the DEGs of these two molecular subtypes which might be able to help finding potential therapeutic target genes in HCC. Using R software, we obtained 1156 up-DEGs and 322 down-DEGs (group 1 vs. group 2), and the heatmap and volcano map of these DEGs were presented in **Figure 4A**, **4B**, respectively. The gene ontology (GO) analyses including biological processes (BP), molecular functions (MF), and cellular compartments (CC) were then carried out, and the results suggested that these DEGs were correlated with metabolism, DNA replication activity and chromosome (**Figure 4C-E**). The KEGG enrichment analysis indicated that these DEGs were related with DNA replication, ECM-receptor interaction, Cell cycle, Bile secretion, PPAR signaling pathway and Steroid hormone biosynthesis (**Figure 4F**).

The analyses of clinical information' difference and DEGs' expression in the two molecular subtypes

In addition, we investigated the available clinical data in search of a connection between this

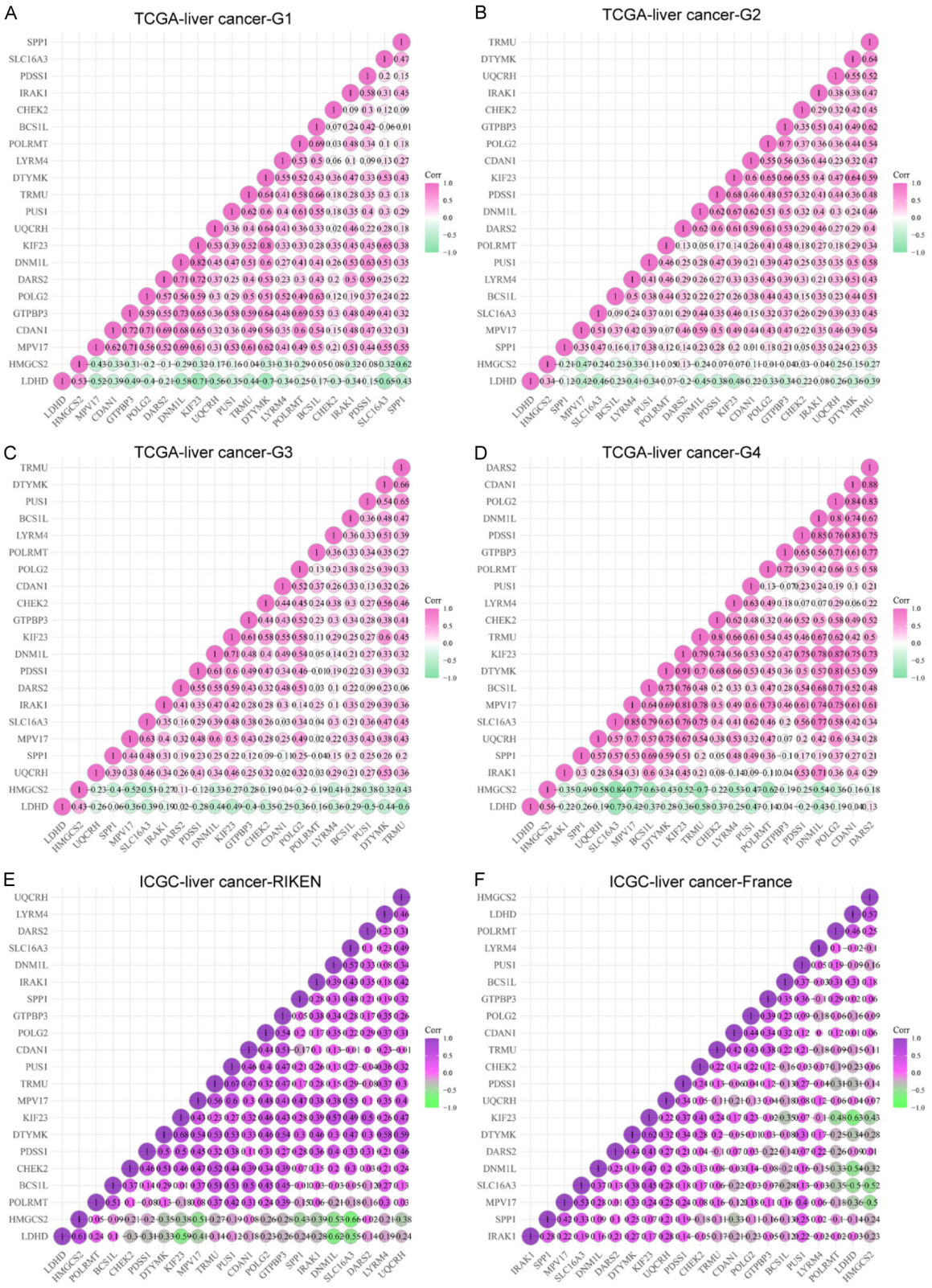

Figure 2. DEGs correlation analysis in HCC. A-D. The heatmaps of DEGs correlation in four grades (grade 1, grade 2, grade 3 and grade 4) of HCC samples based on TCGA database. E. The heatmap of DEGs correlation in ICGC-liver cancer-RIKEN sub-database. F. The heatmap of DEGs correlation in ICGC-liver cancer-France sub-database.

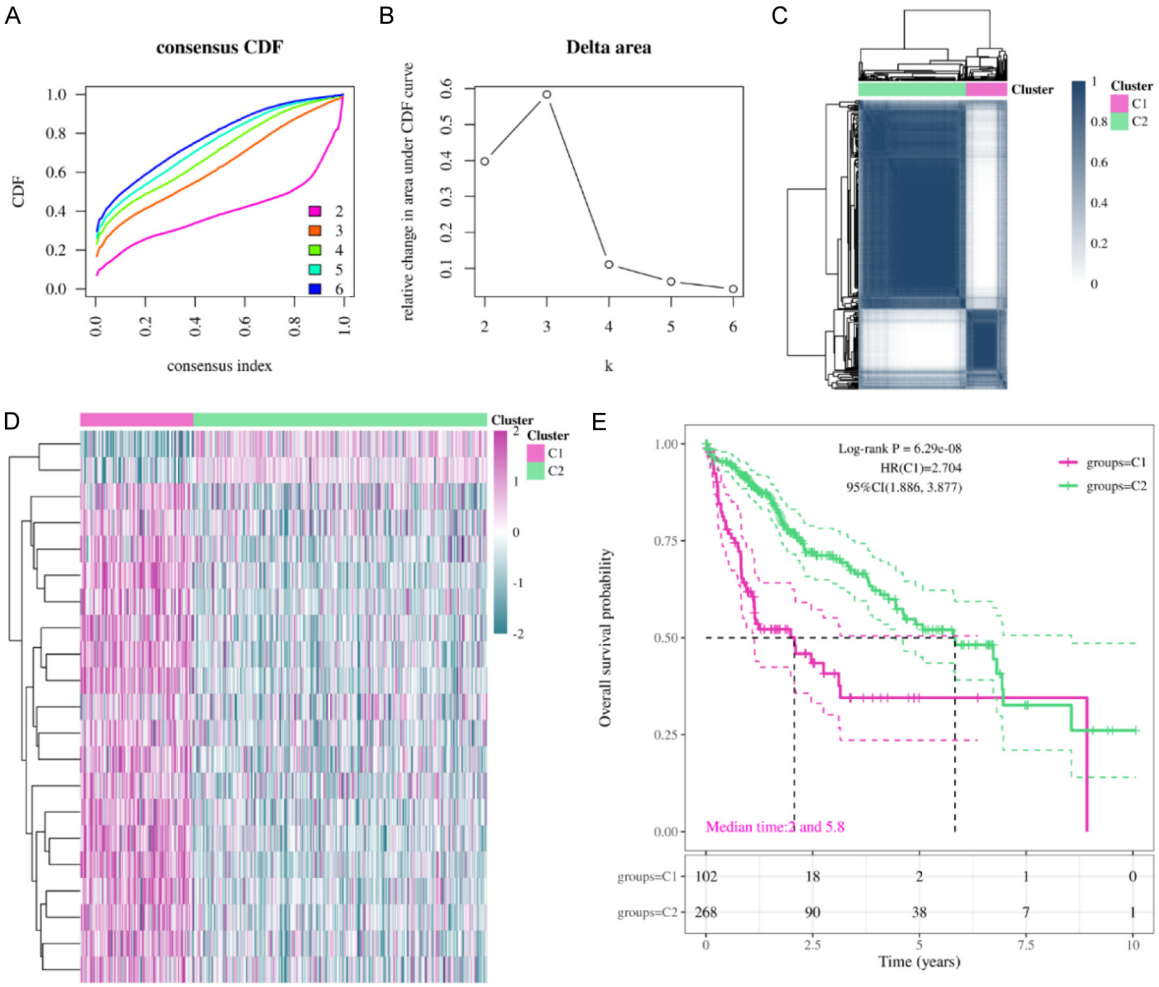

Figure 3. The molecular subtypes of HCC identification based on DEGs. A. The cumulative distribution function (CDF) curves in consensus cluster analysis. B. Area under the cumulative distribution function versus k = 2-6. C. The consensus score matrix of all samples when k = 2. D. The heatmap related to the consensus matrix for k = 2. E. The overall survival (OS) analysis of the two groups. C1 group: 103 HCC samples; C2 group: 268 HCC samples.

data and the genetic subtypes of HCC. According to our results, there were significantly different between the two HCC molecular subtypes in pT stage, pTNM stage and grade, while other clinical characters had no notable difference between the two HCC molecular subtypes (Supplementary Figure 2A-K). Additionally, we also evaluated the expression of the above 21 overlap DEGs in the two HCC molecular subtypes, trying to examine whether the 21 overlap DEGs' expression was similar in the two HCC molecular subtypes when compared with that in TCGA-LIHC samples and corresponding adjacent normal tissues. Interestingly, we found that the expression of the 19 overlap up-DEGs was higher in group 1 (G1, 103 HCC samples), while the 2 overlap down-DEGs' expression was lower in group 1 when compared with that in group 2 (G2, 268 HCC samples) (Supplementary Figure 3A). Moreover, the genetic alteration of the two HCC molecular subtypes were assessed, and the waterfall plots suggested that 81.63% samples had genetic changes in group 1, and 74.23% samples had genetic alterations in group 2 (Supplementary Figure 3B and 3C).

Immune analysis of the two HCC molecular subtypes

Next, we sought to investigate the immune different of the two HCC molecular subtypes. Therefore, we first employed CIBERSORT score to evaluate the difference of multiple types of

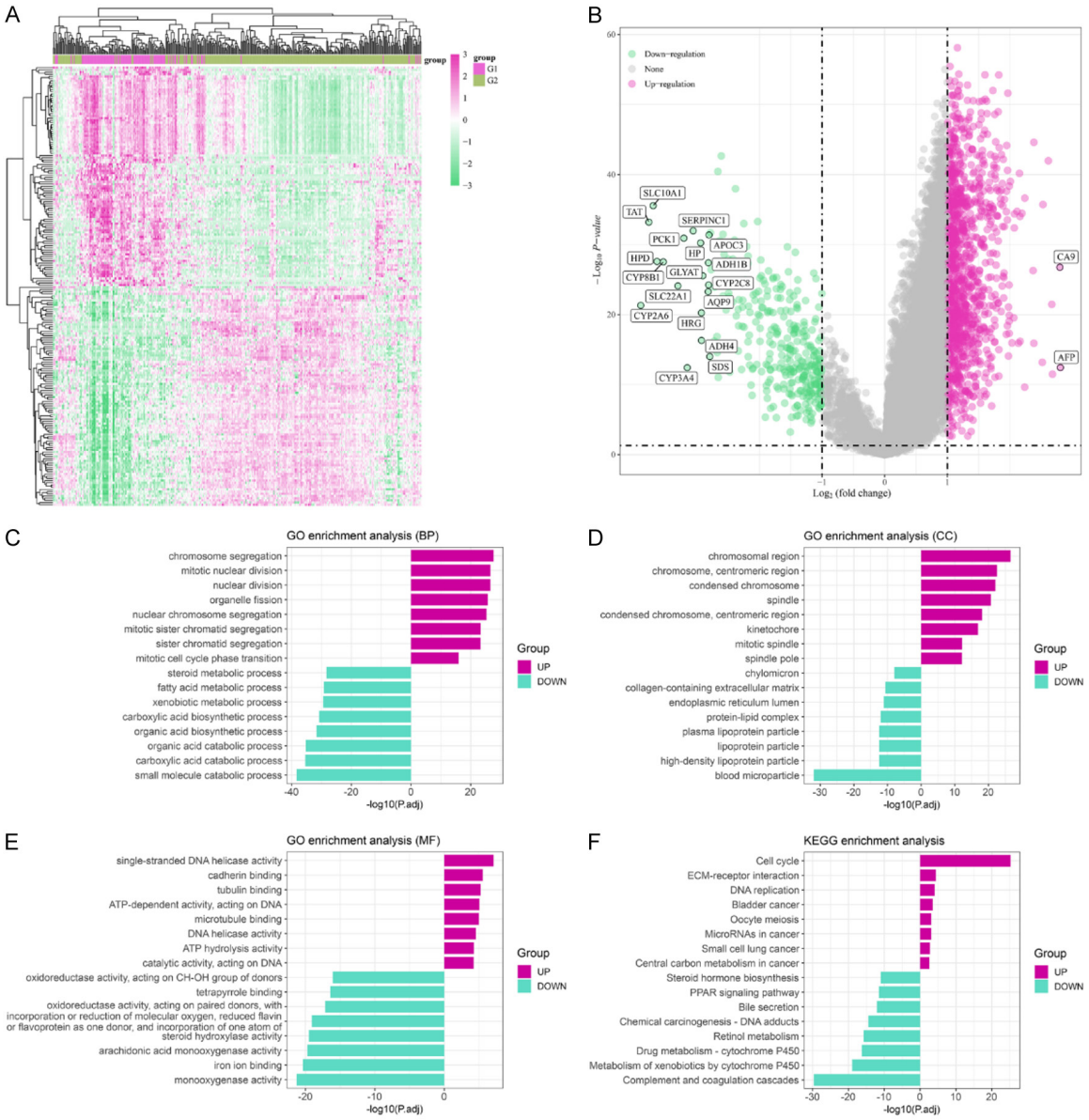

Figure 4. Screening DEGs in the two HCC molecular subtypes and functional enrichment analysis. A. Heatmap of the DEGs in the two HCC molecular subtypes. B. Volcano map. C-E. Gene ontology (GO) analysis. F. KEGG analysis.

immune cells between the two HCC molecular subtypes samples. According to our data, B cell naive, B cell memory, T cell follicular helper, T cell regulatory (Tregs), Monocyte and Macrophage M0 were significantly different in the two HCC molecular subtypes (Supplementary Figure 4A). Subsequently, the expression of the immune checkpoints was also assessed, and the results showed that the expression of CTLA4, HAVCR2, LAG3, PDCD1 and TIGIT was obviously higher in group 1 than that in group 2 (Supplementary Figure 4B). Afterwards, the immune networks of the above 21 DEGs were also constructed respectively in the two HCC molecular subtypes (Supplementary Figure 4C and 4D).

Construction of the lactate-related genes prognostic model

Considering the above analysis had suggested that the 21 overlap DEGs were closely related with HCC survivals, we thereby performed the LASSO regression to develop the prognostic signature based on the 21 overlap DEGs in HCC. The coefficient of 21 overlap DEGs was

presented in Supplementary Figure 5A. The model can achieve the best fit when 9 of 21 DEGs were included (Supplementary Figure 5B). The formula used for risk score computation was as follows: Riskscore = (0.1526)*DTYMK + (0.0313)*IRAK1 + (0.1487)*POLRMT + (0.0422)*MPV17 + (0.1525)*UQCRH + (0.1712)*PDSS1 + (0.0389)*SLC16A3 + (0.0506)*SPP1 + (-0.0163)*LDHD. Based on the risk score model's median threshold, 371 HCC patients were divided into low- and high-risk subgroups, and the 9 genes' heatmap in HCC was also generated (Supplementary Figure 5C). In addition, patients classified as low risk had considerably longer OS than those classified as high risk, as shown by Kaplan-Meier analysis (Supplementary Figure 5D). Besides, using a receiver operating characteristic (ROC) study that took into account the passage of time, we determined how well the prognostic model performed. The area under the ROC curve (AUC) for 1-, 3-, and 5-year OS was 0.784, 0.706, and 0.728, respectively (Supplementary Figure 5E).

Gene Set Variation Analysis (GSVA) of the 9 prognostic lactate-related genes

Since the above analyses established 9 genes prognostic model in HCC, we next sought to use the 9 genes (DTYMK, IRAK1, POLRMT, MPV17, UQCRH, PDSS1, SLC16A3, SPP1, LDHD) as a gene set to investigate their expression and functions in pan-cancers and HCC. The GSVA score was calculated through the R software package "GSVA" based on GSCA database. The GSVA score is positively correlated with the expression of the gene set, and we found that the 9 gene set had high GSVA score in tumor samples than that of the normal tissues across pan-cancers (Supplementary Figure 6A). In addition, the GSVA score in stages (including the pathologic stage, the clinical stage, igcccg stage and masaoka stage) of pan-cancers was also investigated (Supplementary Figure 6B). Furthermore, the correlation of the GSVA score and pathway activity was also studied, and the data suggested that the 9 gene set was positively correlated with apoptosis, cell cycle and EMT in most TCGA cancer types (Supplementary Figure 6C). Besides, the survivals (including OS, PFS, DSS and DFI) between high and low GSVA score in pan-cancers were further evaluated, and the results demonstrated that higher GSVA score had lower OS, PFS, DSS and DFI in many cancer types especially in CHOL, HNSC, KIRC, LGG, LIHC, LUAD and MESO (Supplementary Figure 6D). The detailed OS, PFS, DSS and DFI analyses of the high and low GSVA score in TCGA-LIHC were presented in Supplementary Figure 7A-D, respectively. Finally, the correlation between GSVA score and many kinds of signalings were studied, and we found that GSVA score was positively relevant with Cell Cycle, Apoptosis and EMT pathways, while negatively correlated with Hormone AR, DNA Damage Response, Hormone ER, PI3K/AKT, TSC/mTOR, RAS/MAPK and RTK signalings in HCC (Supplementary Figure 7E).

The mRNA expression, protein levels, methylation, SNV and CNV of POLRMT in pan-cancers

Given that the above analyses revealed that the lactate-related genes, especially the 9 prognostic model genes, were closely related to HCC cells functions or tumor-related signalings, we further selected POLRMT, a mitochondrial DNA-directed RNA polymerase which is closely relevant with cancer cell proliferation, invasion and metabolism, to further investigate whether it is a potential target in HCC and its functions were remained unclear in HCC [20]. The mRNA levels and protein expression across cancer types were respectively explored by using TIMER 2.0 database and HPA database (Supplementary Figure 8A and 8B). In addition, the methylation landscape of POLRMT across cancers were investigated by using GSCA database and the data suggested that POLRMT was low mehylation in kinds of cancers including BLCA, BRCA, COAD, DLBC, LUAD, LUSC, PRAD, STAD and TGCT (Supplementary Figure 8C). Furthermore, data from the SNV study using GSCA database showed that the mutation frequency of POLRMT was notably high in UCEC, COAD, SKCM, STAD and CESC (Supplementary Figure 8D). The CNV of POLRMT across cancers was also evaluated using GSCA database, and the pie plots demonstrated that POLRMT had heterogeneous amplification in ACC, GBM, TGCT, COAD and LGG, while heterogeneous deletion in OV, UCS, LUAD, BRCA, STAD, SKCM and ESCA (Supplementary Figure 8E).

Immune infiltration analyses of POLRMT in pan-cancers

We next attempted to investigate the correlation of POLRMT with immune infiltration in TCGA cancers using CIBERSORT algorithm and

XCELL algorithm. Data from the CIBERSORT algorithm suggested that POLRMT was positive correlation with γδ T cells, CD4+ T cells, Neutrophil, Monocyte, Macrophage (Supplementary Figure 9A). Another algorithm XCELL also revealed that POLRMT was positively relevant with the majority of immune cells including immune score, Tregs, CD8+ T cells, Neutrophil, Monocyte, Macrophage, CD4+ T cells in pan-cancers, which was corresponding with the results of CIBERSORT algorithm (Supplementary Figure 9B). Next, we aimed to determine if POLRMT was related to tumor mutation burden (TMB) and microsatellite instability (MSI) in pan-cancers, as TMB has become a predictive indicator for tumor immunotherapy and MSI is a genetic change that has been shown to be closely associated with tumor prognosis. The data suggested that POLRMT high expression was obviously correlated with TMB and MSI in most TCGA cancer types (Supplementary Figure 9C and 9D).

The mRNA expression, protein levels, methylation, SNV, CNV and immune networks of POLRMT in HCC

The results from the GEPIA database displayed that POLRMT mRNA levels were higher in HCC tumor tissues than that of the adjacent normal tissues (Supplementary Figure 10A). Similar results were also observed using the ICGC-liver cancer-RIKEN sub-database (Supplementary Figure 10B). The protein levels of POLRMT were also higher in HCC tumor tissues when analyzed by UALCAN database (Supplementary Figure 10C). Besides, the immunohistochemistry based on HPA database of POLRMT in HCC tumor samples also demonstrated that POLRMT expressed in HCC tumor tissues (Supplementary Figure 10D). The overall survival (OS) analysis from UALCAN database and disease free survival (DFS) from GEPIA database proved that high expression of POLRMT had poor OS and PFS in HCC (Supplementary Figure 10E and 10F). Although the somatic mutation rate of POLRMT in HCC was low (0.55%), about one-third of the HCC samples had CNV of POLRMT (Supplementary Figure 10G and 10H). Besides, the immune networks of POLRMT in HCC were further assessed by using CIBERSORT and XCELL algorithms, and the data suggested that POLRMT was closely relevant with multiple types of immune cells in HCC (Supplementary Figure 11).

Interacting network of POLRMT and prognostic model construction based on POLRMT interacting genes

We utilized the GeneMania database to look for genes or proteins that potentially interact or co-express with POLRMT in order to learn more about the complex network of interactions between POLRMT and other genes. The interacting network was presented in Supplementary Figure 12A, and the interacting genes were: TFB2M, TFAM, MTERF1, TFB1M, MTRES1, TEFM, MRPL58, COX10, HECW2, TARDBP, MRPL12, HIF1A, SIRT7, RUVBL2, ATP5F1D, MLH1, PNPLA6, POLR2E, PKN1, TRIM28. Afterwards, we employed the LASSO regression to develop a prognostic signature based on the 20 POLRMT interacting genes. The coefficient of 20 POLRMT interacting genes was presented in Supplementary Figure 12B. The model can achieve the best fit when 10 of 20 genes were included (Supplementary Figure 12C). The formula used for risk score computation was as follows: riskscore = (0.007)*TFB2M + (0.1538)*MTRES1 + (0.0049)*MRPL58 + (-0.2458)*HECW2 + (0.3682)*TARDBP + (0.1447)*HIF1A + (0.0693)*SIRT7 + (0.0522)*RUVBL2 + (0.2796)*POLR2E + (0.0402)*TRIM28. Subsequently, the TCGA-LIHC samples were divided into low- and high-risk subgroups according to the above riskscore. The heatmap of the 10 genes, and patients' alive and dead status were presented in Supplementary Figure 12D. Then, the overall survival of the low- and high-risk subgroups was analyzed and the patients with high-risk had poor OS than that of the patients with low-risk (Supplementary Figure 12E). Additionally, the area under the ROC curve (AUC) for 1-, 3-, and 5-year OS was also calculated, and the value was respectively 0.738, 0.682 and 0.704 (Supplementary Figure 12F).

Real-time PCR assays detecting the POLRMT expression in HCC cells under various conditions

Since the above studies had uncovered the potential important roles of POLRMT in HCC, we next attempted to carry out experiments to verify whether POLRMT had critical effects on HCC tumor cells functions. To that purpose, we first employed CCLE database to explore the POLRMT expression in kinds of HCC cell lines. As shown in **Figure 5A**, nearly all the 25 HCC

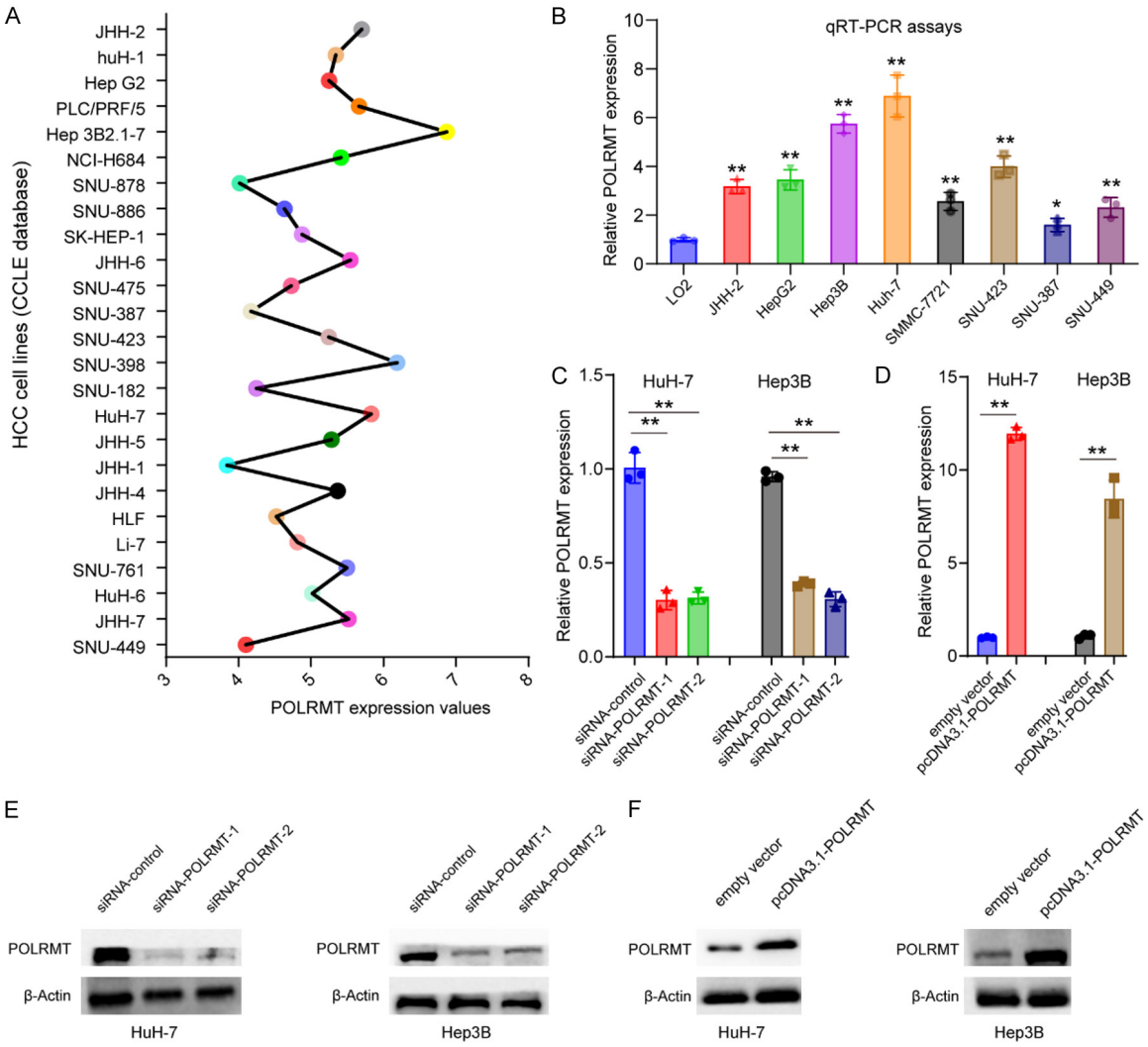

Figure 5. The POLRMT expression in HCC cells. (A) POLRMT expression in HCC cell lines based on CCLE database. (B) qRT-PCR assays. (C and D) qRT-PCR assays and (E and F) Western blot assays evaluating the POLRMT expression in cells treated with POLRMT siRNAs and overexpressing plasmids.

cell lines highly expressed POLRMT. Next, we performed qRT-PCR assays to assess the POLRMT expression in LO2, JHH-2, HepG2, Hep3B, Huh-7, SMMC-7721, SNU-423, SNU-387 and SNU-449 cells. The results proved that POLRMT expression was much higher in Hep3B and Huh-7 cells when compared with other HCC cell lines or normal liver cell line LO2 (**Figure 5B**). Hence, we next selected Huh-7 and Hep3B cells for the following experiments. Subsequently, the siRNAs targeting POLRMT (siRNA-POLRMT-1 and siRNA-POLRMT-2) were obtained and plasmids over-expressing POLRMT (pcDNA3.1-POLRMT) were constructed. These siRNAs and plasmids were transfected into Huh-7 and Hep3B cells, respectively. The data from the qRT-PCR assays and western blot indicated that siRNA-POLRMT-1 and siRNA-POLRMT-2 were able to significantly reduce the POLRMT expression (**Figure 5C** and **5E**) and pcDNA3.1-POLRMT could obviously promote the expression of POLRMT (**Figure 5D** and **5F**).

The silence of POLRMT affects HCC cells functions and energy metabolism

Next, CCK-8 assays were carried out to assess the affections of POLRMT on HCC cellular viability when the cells were transfected with siRNA-POLRMT-1, siRNA-POLRMT-2 or pcDNA3.1-POLRMT. The results demonstrated that the POLRMT depletion dramatically reduced the proliferation of Huh-7 and Hep3B cells, while

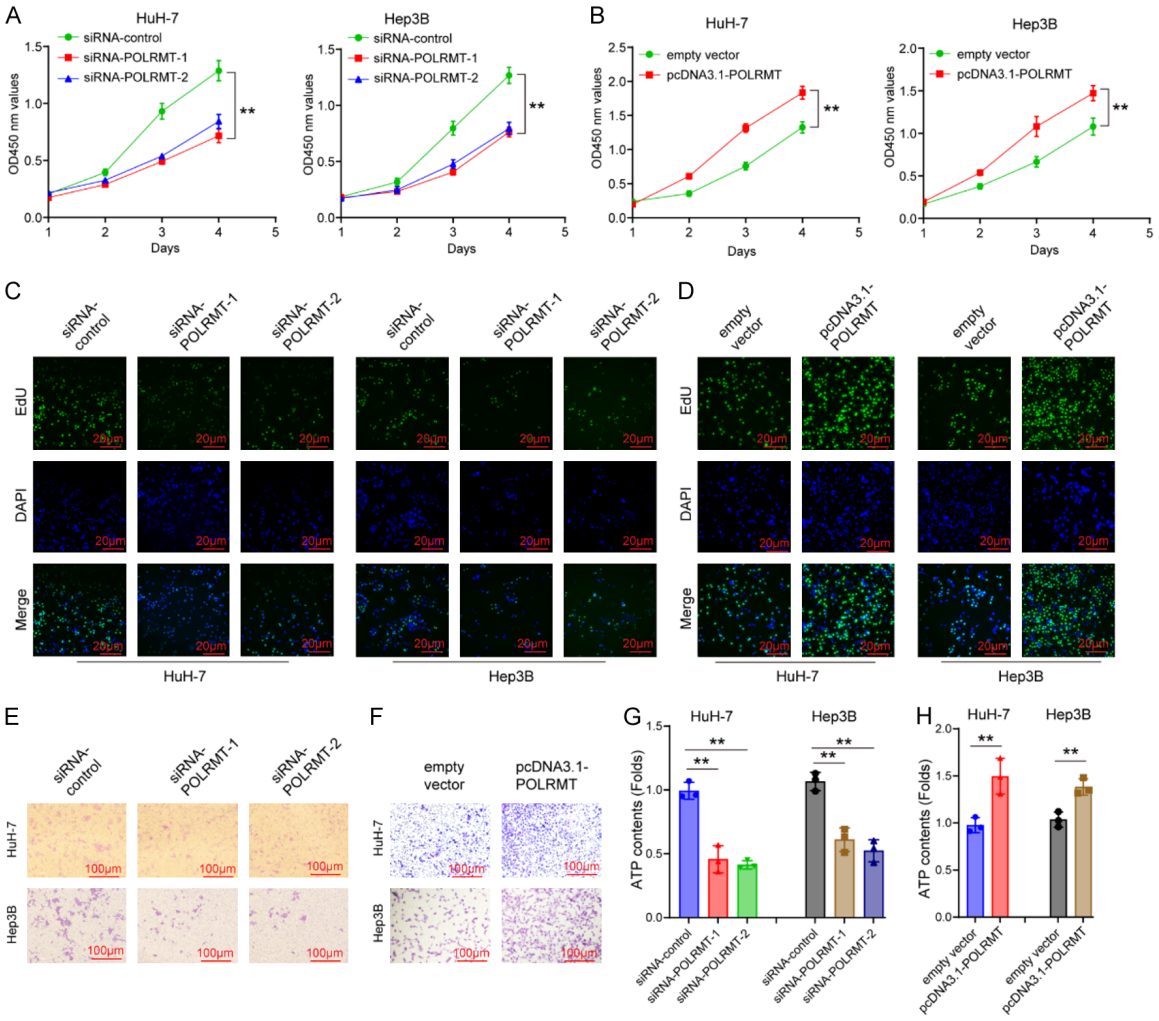

Figure 6. The affection of POLRMT on HCC cell growth and migration. A and B. CCK-8 assays. C and D. EdU staining. E and F. Transwell migration assays. G and H. Silencing POLRMT expression remarkably decreased the ATP contents in Huh7 and Hep3B cells, while promoting POLRMT expression increased the ATP contents.

the POLRMT overexpression notably increased the cellular proliferation (**Figure 6A** and **6B**). Then, the EdU examination was also performed to assess the cellular proliferation of HCC cells under various treatment. The data indicated that elevated expression of POLRMT significantly increased the proliferative HCC cells, while silencing POLRMT expression obviously reduced the number of HCC cells (**Figure 6C** and **6D**). Afterwards, the transwell chambers were utilized for the determination of the migration abilities of HCC cells after POLRMT was knocked down or accelerated expression. As the results displayed in **Figure 6E** and **6F**, impeding the POLRMT expression significantly attenuated the migration of both Huh-7 and Hep3B cells, while restoring the POLRMT expression was able to enhance the HCC cells migration. Since previous reports had indicated that POLRMT depletion was able to disrupt mitochondrial functions, we thereby next measured the ATP contents in HCC cells after POLRMT was knocked down. The data demonstrated that silencing POLRMT expression remarkably decrease the ATP contents in Huh7 and Hep3B cells, while enhancing POLRMT expression obviously increased the ATP contents (**Figure 6G** and **6H**).

Identification of the differentially expressed genes in POLRMT high and low expression HCC samples

Next, the 371 HCC samples based on TCGA database was separated into POLRMT high

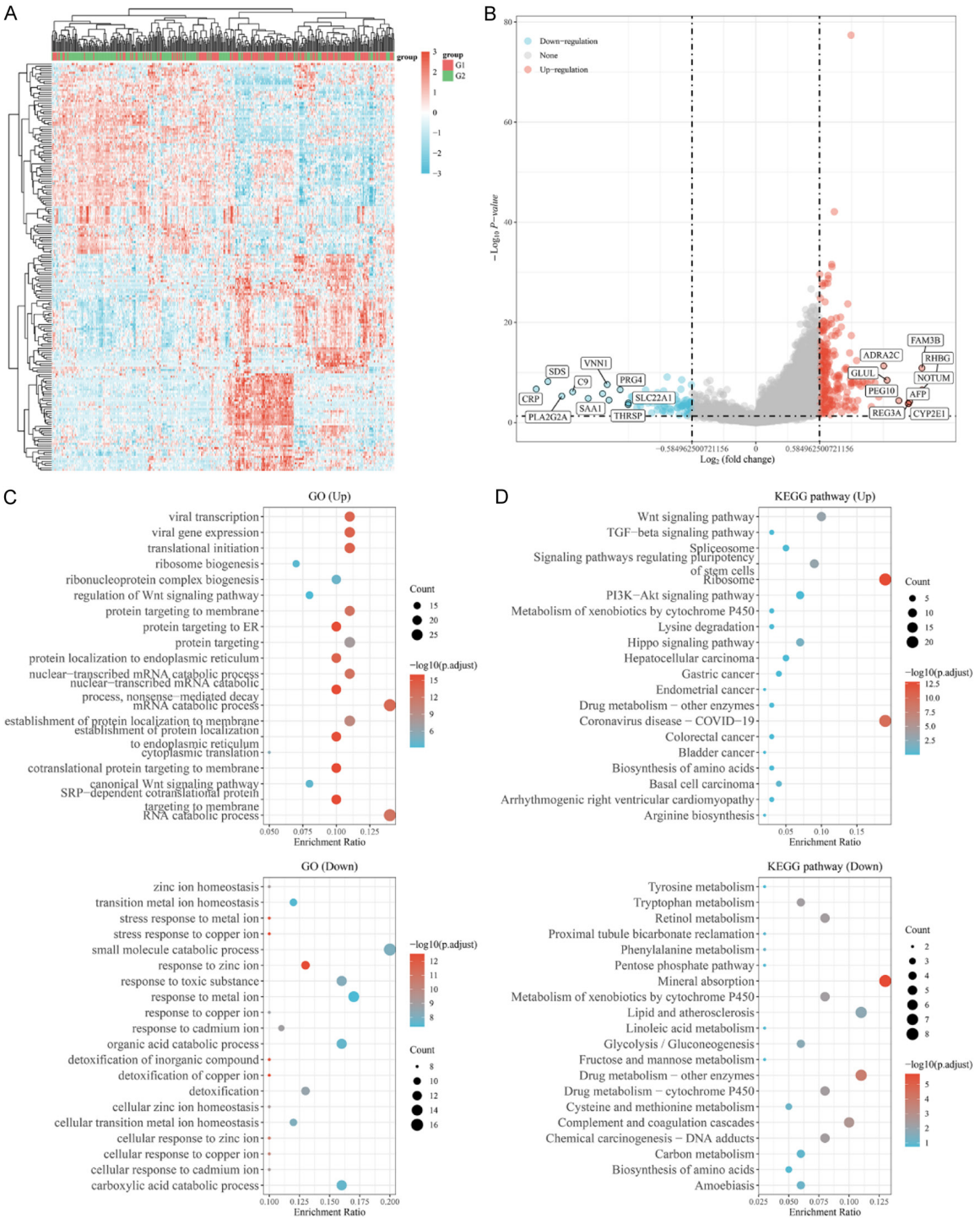

Figure 7. The DEGs identification in POLRMT high and low expression HCC samples. A. Heatmap. B. Volcano plot. C. GO analysis. D. KEGG analysis.

(G1: 186 HCC samples) and low (G2: 185 HCC samples) expression group, and the DEGs (221 up-regulated genes and 88 low-regulated genes when G1 compared with G2) were verified. The heatmap and volcano plot were respectively shown in **Figure 7A** and **7B**. Subsequently, the functional analyses were conducted including GO and KEGG analyses. The GO analysis revealed that the DEGs were associated with the regulation of Wnt signaling

pathway, ribonucleoprotein complex biogenesis, ribosome biogenesis, translational initiation, viral gene expression, viral transcription, response to zinc ion, small molecule catabolic process, stress response to copper ion, stress response to metal ion, transition metal ion homeostasis and zinc ion homeostasis (**Figure 7C**). The KEGG analysis revealed that these DEGs were correlated with Wnt signaling pathway, TGF-beta signaling pathway, Spliceosome, Signaling pathways regulating pluripotency of stem cells, Ribosome, and kinds of metabolism (**Figure 7D**).

POLRMT modulated Wnt/β-Catenin signaling in HCC cells

To further uncover the potential molecular mechanism by which POLRMT regulated the HCC tumor cells functions, we next conducted the correlation analysis between 150 genes relevant with Wnt signaling, because numerous reports had demonstrated that Wnt signaling played essential roles in modulation tumor development and progression. The heatmaps of the correlation between POLRMT and 150 genes relevant with Wnt signaling were generated by the R software package "ggstatsplot", and the data proved that POLRMT was positively correlated with most of the Wnt signaling-related genes (**Figure 8A**). In addition, the detail analyses using GSCA database further certified that POLRMT was notably positively correlated with three critical Wnt/β-Catenin signaling related genes including CTNNB1, CCND1 and c-MYC (**Figure 8B-D**). Finally, we carried out western blot assays to determine the expression of Wnt/β-Catenin signaling related critical factors in HCC cells when POLRMT was depleted or overexpressed. The results suggested that impeding the POLRMT expression significantly attenuated the protein levels of β-Catenin, Cyclin D1 and c-Myc in both Huh-7 and Hep3B cells, while restoring the POLRMT expression was able to remarkably enhance these three protein expression in HCC cells (**Figure 8E** and **8F**).

IC50 scores analysis of drugs targeting HCC in POLRMT high and low expression groups

Considering our above studies had indicated that POLRMT might be a potential target in HCC, we next sought to investigate the IC50 scores of kinds of drugs used in liver cancer treatment based on POLRMT high and low expression. According to the data from GDSC database (https://www.cancerrxgene.org/), the IC50 scores of Talazoparib, Gefitinib, Cisplatin, Trametinib and Dasatinib in POLRMT high expression group (G1) were higher than that in POLRMT low expression group (G2), while Crizotinib, Gemcitabine, Sorafenib, Tamoxifen, 5-Fluorouracil, and Ruxolitinib in POLRMT high expression group were lower than that in POLRMT low expression group, and there were no significant difference of other drugs between POLRMT high and low expression groups (Supplementary Figure 13).

Discussion

The prognosis of HCC varies depending on individual factors such as the patient's health status, the type of cancer, the stage of the disease, and the treatment methods used. Generally, the prognosis for HCC is relatively poor, especially for patients diagnosed at an advanced stage [21]. HCC often presents with no noticeable symptoms in its early stages, leading to late diagnosis in many cases. Early diagnosis and timely treatment can improve the prognosis [22, 23]. For early-stage HCC patients, if the tumor is confined to the liver and has not spread to other parts of the body, surgical resection may be the preferred treatment option, which generally offers a better prognosis [24, 25]. However, for patients with advanced HCC, where the disease has already spread to other organs, the treatment becomes more challenging, resulting in a poorer prognosis. In recent years, there have been some positive advancements in HCC treatment, including the use of immunotherapy and targeted therapy. These novel treatment approaches are still under research and application, providing more treatment options for patients [26, 27]. However, for advanced HCC cases, the cure rate remains relatively low. Identification of novel biomarker for HCC patients is very important. In this study, our attention focused on lactate-related genes.

Lactate metabolism and HCC are closely related. Lactic acid metabolism is an essential biochemical process within cells, closely associated with energy production and cell survival [28]. When cells need energy, they metabolize glucose (glycolysis) to produce lactic acid, a

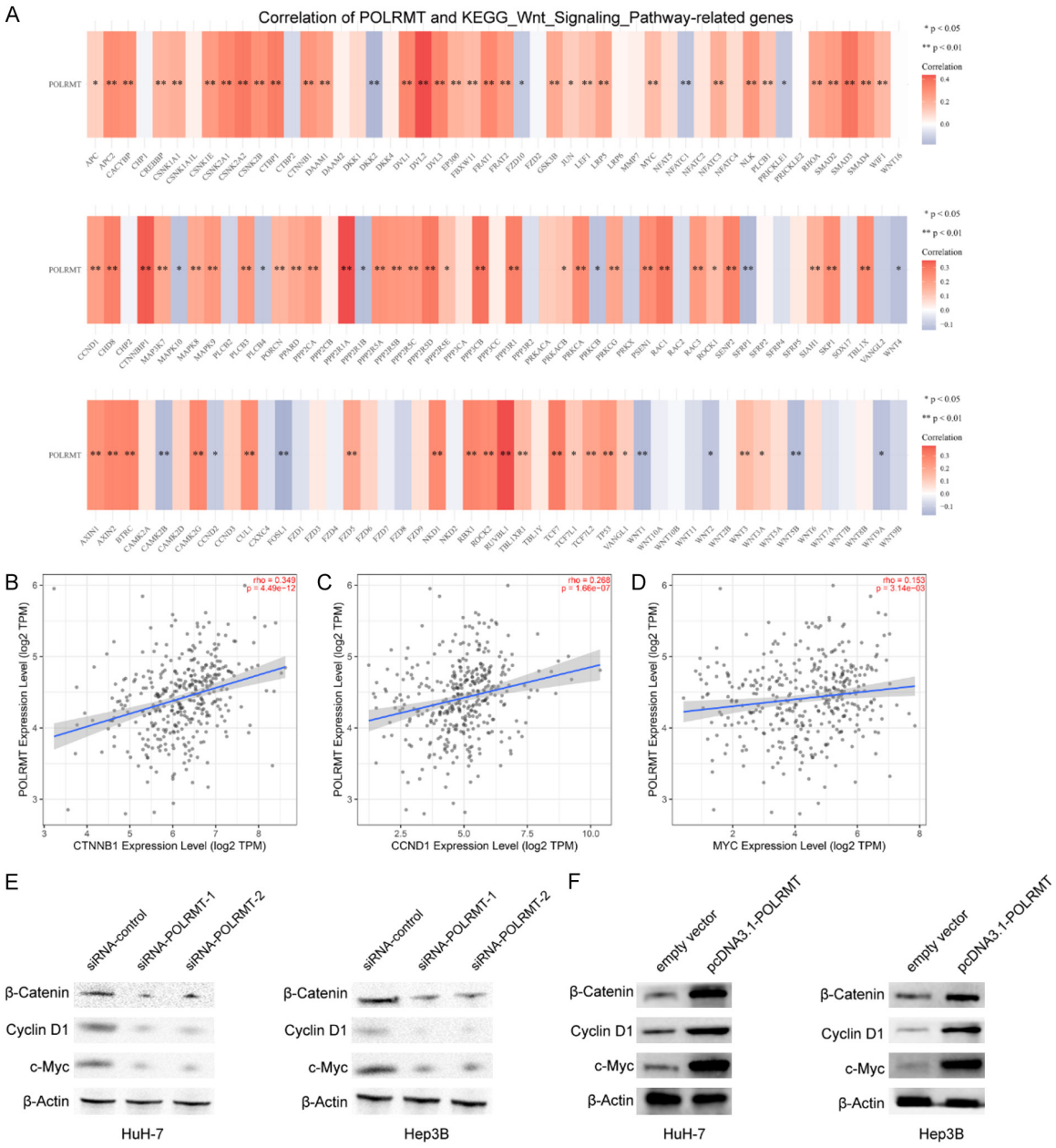

Figure 8. POLRMT affects Wnt/β-Catenin signaling in HCC. A. The correlation analysis between POLRMT and 150 genes relevant with Wnt signaling. B-D. The correlation analysis between POLRMT and CTNNB1, CCND1 or c-MYC, respectively. E, F. Western blot assays detect the protein levels of β-Catenin, Cyclin D1 and c-Myc in Huh-7 and Hep3B cells after treatment, respectively.

process known as anaerobic metabolism. Under normal conditions, the produced lactic acid is transported to the liver through the body's lactate clearance system, where it is further converted into energy or re-synthesized into glucose (gluconeogenesis) [29, 30]. However, in certain circumstances, the cell's metabolic processes may become abnormal, leading to excessive production of lactic acid, surpassing the liver's metabolic capacity, resulting in lactic acid accumulation (lactic acidosis). This phenomenon is particularly common in tumor cells. Tumor cells often proliferate at an unusually rapid rate, and to meet their energy demands, they frequently rely on anaerobic pathways (i.e., lactic acid production pathway) to generate large amounts of energy [15, 31]. In this study, we analyzed TCGA datasets and

identified 21 differentially expressed LRGs that were significantly associated with overall survival in HCC patients. These genes are involved in various important biological processes related to tRNA modification, mitochondrial RNA metabolism, and catalytic activities. Furthermore, they are associated with mitochondrial respiratory chain complexes and terpenoid backbone biosynthesis. These findings suggest that these genes may play crucial roles in HCC development and progression and could potentially serve as therapeutic targets for the treatment of HCC. Then, we sought to explore the mRNA expression, genetic changes, and methylation status of the above-selected 21 DEGs across TCGA cancers. Our findings indicate that the 21 DEGs identified in this study have widespread dysregulation across multiple cancer types, with potential implications in cancer progression and development. These genes may serve as important targets for further investigation and potential therapeutic intervention in pan-cancer studies. In addition, the analysis of the 21 DEGs in HCC across TCGA and ICGC databases revealed consistent positive correlations among up-regulated DEGs in various HCC grades, indicating potential co-regulation during HCC progression. In contrast, down-regulated DEGs (HMGCS2 and LDHD) consistently exhibited negative correlations with other DEGs across different HCC grades and databases, implying a distinct regulatory role. However, the correlation patterns showed some variations in the ICGC-liver cancer-France sub-database, suggesting complex heterogeneity within HCC tumor samples.

The immune microenvironment refers to the interaction between immune cells, inflammatory factors, cytokines, and other immune-related components with tumor cells in the tumor microenvironment [32]. In HCC, the immune microenvironment plays a crucial role, influencing tumor development and treatment outcomes. The immune microenvironment in HCC typically includes two states: immune suppression and immune activation. Immune suppression indicates the presence of numerous immune inhibitory cells, such as regulatory T cells (Tregs), tumor-associated macrophages (TAMs), and immune-suppressive cytokines (e.g., TGF-β and IL-10) [33, 34]. These immune inhibitory factors contribute to suppressing the immune system's attack on tumor cells, enabling tumors to evade immune clearance and promoting tumor proliferation and metastasis [35, 36]. On the other hand, immune activation state signifies the presence of active immune cells, such as cytotoxic T lymphocytes (CTLs) and natural killer (NK) cells, surrounding the tumor. These immune cells recognize and attack tumor cells, exerting an anti-tumor effect. Immune activation helps to limit tumor growth and dissemination, facilitating tumor regression. The immune microenvironment in HCC significantly impacts tumor treatment and prognosis. Some immunotherapies, such as immune checkpoint inhibitors, have shown promising results in HCC treatment. However, due to the complexity of the immune microenvironment in HCC, current treatment outcomes are still limited. In this study, we found that the 21 DEGs were able to distinguish the TCGA-LIHC samples into two molecular subtypes, C1 and C2, and there was a significant difference in overall survival between these subtypes. These findings suggest that these DEGs might play a crucial role in determining the molecular heterogeneity of HCC and have potential implications for prognostic stratification and targeted therapies in HCC patients. Besides, we observed that the two HCC molecular subtypes exhibit differences in immune cell composition and immune checkpoint expression, indicating potential variations in the tumor immune microenvironment and immune response between the subtypes. These results could have important implications for understanding the immune characteristics of different HCC subtypes and may help guide the development of targeted immunotherapies for HCC patients.

Then, we performed the LASSO regression to develop the prognostic signature based on the 21 overlap DEGs in HCC. Finally, we developed a novel prognostic model using nine genes, including DTYMK, IRAK1, POLRMT, MPV17, UQCRH, PDSS1, SLC16A3, SPP1 and LDHD. Based on these analysis results, the study found that among 371 HCC patients, they were classified into low-risk and high-risk subgroups using a risk score model. Patients in the low-risk group exhibited significantly better overall survival (OS) compared to those in the high-risk group. Further time-dependent receiver operating characteristic (ROC) analysis evaluated the predictive model's efficacy, with AUC values of 0.784, 0.706, and 0.728 for 1-year, 3-year, and

5-year OS, respectively. These findings indicated that the prognostic model effectively predicts the survival of HCC patients and provides valuable information for risk stratification. GSVA is a method used for gene expression data analysis. It is a common technique in bioinformatics, utilized to explore the expression variation of gene sets across different samples. Traditional gene expression analysis typically focuses on individual genes for statistical analysis, whereas GSVA aims to analyze predefined gene sets (e.g., pathways, biological processes, or functional modules). In this study, in pan-cancers, the expression levels of this set of nine genes (represented by GSVA scores) were generally higher in tumor samples compared to normal tissues. This suggests that these genes may play important roles in various types of cancer. In different stages of cancer, the GSVA scores of the set of nine genes also show some variations. This may be associated with the different stages of tumor development and the diverse biological characteristics of the tumors. In HCC, the GSVA scores of the set of nine genes were positively correlated with signaling pathways such as the cell cycle, apoptosis, and epithelial-mesenchymal transition (EMT). However, they were negatively correlated with signaling pathways like hormone AR (androgen receptor), DNA damage response, hormone ER (estrogen receptor), PI3K/AKT, TSC/mTOR, RAS/MAPK, and RTK (receptor tyrosine kinase). These findings may provide crucial clues for studying the underlying mechanisms of HCC development. These analysis results emphasized the significance of these nine genes in various types of cancer, particularly in HCC.

Out of the nine prognostic LRGs, we zeroed in on POLRMT because it is a nuclear-encoded RNA polymerase that is essential for the production of mitochondrial genes that code for components of oxidative phosphorylation complexes. POLRMT encodes RNA polymerase, which synthesizes various mitochondrial RNAs in the mitochondria, including mRNA that codes for mitochondrial proteins. These mitochondrial proteins are essential for cellular lactate metabolism and energy production processes. In certain cases, mutations or abnormalities in the POLRMT gene can lead to mitochondrial dysfunction, affecting cellular energy metabolism and lactate production [37]. Mitochondrial dysfunction can result in the accumulation of lactate, a condition known as lactic acidosis [38]. Lactic acidosis is a rare but severe genetic mitochondrial disorder, and its symptoms may include muscle weakness, fatigue, rapid breathing, and neurological issues. Growing studies indicated that the expressions of POLRMT was related to various cancers, including breast cancer, acute myeloid leukemia, osteosarcoma and skin squamous cell carcinoma [39-42]. However, the expression and function of POLRMT in HCC were rarely reported. In this study, we found that the expression of POLRMT was distinctly increased in HCC specimens compared with non-tumor specimens. We explored the mRNA and protein expression levels, DNA methylation status, SNV frequency, and CNV of POLRMT across various types of cancer, using various bioinformatics databases. POLRMT may play a significant role in various types of cancer, especially in HCC. The methylation level, mutation frequency, and copy number variation of POLRMT vary among different cancers, which might reflect its complex role in cancer development and progression. Analysis of OS and DFS in HCC patients revealed that high expression of POLRMT was associated with poor survival and disease recurrence. While the somatic mutation rate of POLRMT in HCC was low (0.55%), approximately one third of the HCC samples showed CNV of POLRMT. Furthermore, using CIBERSORT and XCELL algorithms, we assessed the immune networks of POLRMT in HCC and found that POLRMT was closely associated with multiple types of immune cells in HCC. Overall, these data suggest that POLRMT may play a crucial role in HCC, correlating with disease progression and patient survival, and may interact with the tumor's immune environment. These findings supported the potential of POLRMT as a possible therapeutic target in HCC. Finally, we performed functional assays and confirmed that knockdown of POLRMT distinctly suppressed the proliferation and migration of HCC cells, suggesting it as a tumor promotor in HCC.

The Wnt signaling pathway is a crucial intercellular signal transduction system involved in many biological processes, such as cell proliferation, differentiation, polarity maintenance, and embryonic development [43]. The Wnt signaling pathway is closely associated with HCC. Under normal physiological conditions, the Wnt signaling pathway plays a crucial role in maintaining the normal function and regeneration of liver tissue [44, 45]. However, when this path-

way undergoes abnormal activation or dysregulation, it can become a key driving factor in the occurrence and development of HCC. Enhanced activity of the Wnt signaling pathway not only promotes tumor formation but may also render existing tumors more invasive and prone to metastasis [46, 47]. Some studies suggest that the Wnt signaling pathway may be associated with the maintenance of cancer stem cells, a small subset of cells capable of self-renewal and driving tumor growth [48]. To further investigate its potential molecular mechanism, we conducted a correlation analysis between 150 genes associated with the Wnt signaling pathway. We discovered a positive correlation between POLRMT and these Wnt signaling-related genes. This finding suggests that POLRMT might play a significant role in regulating the functions of the Wnt signaling pathway, thereby influencing the development and progression of HCC tumor cells. The influence of POLRMT on Wnt/β-Catenin signaling was further affirmed by our western blot assays, which demonstrated that depletion of POLRMT led to a significant reduction in the protein levels of β-Catenin, Cyclin D1, and c-Myc in Huh-7 and Hep3B HCC cell lines. Conversely, overexpression of POLRMT led to a marked increase in the expression of these three proteins, further strengthening the proposition that POLRMT may act as a regulator of the Wnt/β-Catenin signaling pathway in HCC.

Several caveats should be noted about the present investigation. First, Due to the nature of a retrospective study, gaps in data and biases in sample selection were unavoidable. Second, the potential of POLRMT in HCC progression was not studied in vivo experiments. Thus, findings in this study are waiting for further validation by well-designed, prospective, multicenter studies.

Conclusion

Overall, our study developed a signature for predicting the prognosis of HCC patients based on 9 lactate-related genes; this signature has the potential to open up new avenues of inquiry into the mechanisms of lactic acid metabolism and personalized prognostic predictions as well as provide a new therapeutic target for people with CC. In addition, we confirmed that POLRMT was highly expressed in HCC and its knockdown suppressed the proliferation, migration and energy metabolism of HCC cells via Wnt signaling pathway. Based on the expression of POLRMT in HCC and its role in cell proliferation and migration, further research on the function and regulatory network of POLRMT is warranted to develop more precise treatment methods, particularly focusing on the modulation of the Wnt signaling pathway.

Acknowledgements

This study was supported by Beijing Natural Science Foundation (No. 7202181).

Disclosure of conflict of interest

The authors declare that the research was conducted in the absence of any commercial or financial relationships that could be construed as a potential conflict of interest.

Address correspondence to: Shiyu Du, Department of Gastroenterology, China-Japan Friendship Hospital, No. 2, Yinghua East Road, Chaoyang District, Beijing 100029, P. R. China. E-mail: dushiyu1975@126.com

References

[1] Siegel RL, Miller KD, Fuchs HE and Jemal A. Cancer statistics, 2022. CA Cancer J Clin 2022; 72: 7-33.
[2] Miller KD, Nogueira L, Devasia T, Mariotto AB, Yabroff KR, Jemal A, Kramer J and Siegel RL. Cancer treatment and survivorship statistics, 2022. CA Cancer J Clin 2022; 72: 409-436.
[3] Feng M, Pan Y, Kong R and Shu S. Therapy of primary liver cancer. Innovation (Camb) 2020; 1: 100032.
[4] Lin S, Hoffmann K and Schemmer P. Treatment of hepatocellular carcinoma: a systematic review. Liver Cancer 2012; 1: 144-158.
[5] Medavaram S and Zhang Y. Emerging therapies in advanced hepatocellular carcinoma. Exp Hematol Oncol 2018; 7: 17.
[6] Bang A and Dawson LA. Radiotherapy for HCC: ready for prime time? JHEP Rep 2019; 1: 131-137.
[7] Geh D, Manas DM and Reeves HL. Hepatocellular carcinoma in non-alcoholic fatty liver disease-a review of an emerging challenge facing clinicians. Hepatobiliary Surg Nutr 2021; 10: 59-75.
[8] Strobel EJ, Yu AM and Lucks JB. High-throughput determination of RNA structures. Nat Rev Genet 2018; 19: 615-634.
[9] Rodriguez R and Miller KM. Unravelling the genomic targets of small molecules using high-throughput sequencing. Nat Rev Genet 2014; 15: 783-796.

[10] Pipis M, Rossor AM, Laura M and Reilly MM. Next-generation sequencing in Charcot-Marie-Tooth disease: opportunities and challenges. Nat Rev Neurol 2019; 15: 644-656.
[11] Xu Y and Zhao F. Single-cell metagenomics: challenges and applications. Protein Cell 2018; 9: 501-510.
[12] Scherer F, Kurtz DM, Diehn M and Alizadeh AA. High-throughput sequencing for noninvasive disease detection in hematologic malignancies. Blood 2017; 130: 440-452.
[13] Friedensohn S, Khan TA and Reddy ST. Advanced methodologies in high-throughput sequencing of immune repertoires. Trends Biotechnol 2017; 35: 203-214.
[14] Li X, Yang Y, Zhang B, Lin X, Fu X, An Y, Zou Y, Wang JX, Wang Z and Yu T. Lactate metabolism in human health and disease. Signal Transduct Target Ther 2022; 7: 305.
[15] Brooks GA. The science and translation of lactate shuttle theory. Cell Metab 2018; 27: 757-785.
[16] Apostolova P and Pearce EL. Lactic acid and lactate: revisiting the physiological roles in the tumor microenvironment. Trends Immunol 2022; 43: 969-977.
[17] Barros LF. Metabolic signaling by lactate in the brain. Trends Neurosci 2013; 36: 396-404.
[18] Iscra F, Gullo A and Biolo G. Bench-to-bedside review: lactate and the lung. Crit Care 2002; 6: 327-329.
[19] Ippolito L, Morandi A, Giannoni E and Chiarugi P. Lactate: a metabolic driver in the tumour landscape. Trends Biochem Sci 2019; 44: 153-166.
[20] Kühl I, Kukat C, Ruzzenente B, Milenkovic D, Mourier A, Miranda M, Koolmeister C, Falkenberg M and Larsson NG. POLRMT does not transcribe nuclear genes. Nature 2014; 514: E7-11.
[21] Daniele G, Costa N, Lorusso V, Costa-Maia J, Pache I and Pirisi M. Methodological assessment of HCC literature. Ann Oncol 2013; 24 Suppl 2: ii6-14.
[22] Kallini JR, Gabr A, Salem R and Lewandowski RJ. Transarterial radioembolization with Yttrium-90 for the treatment of hepatocellular carcinoma. Adv Ther 2016; 33: 699-714.
[23] Teng YX, Xie S, Guo PP, Deng ZJ, Zhang ZY, Gao W, Zhang WG and Zhong JH. Hepatocellular carcinoma in non-alcoholic fatty liver disease: current progresses and challenges. J Clin Transl Hepatol 2022; 10: 955-964.
[24] Donisi C, Puzzoni M, Ziranu P, Lai E, Mariani S, Saba G, Impera V, Dubois M, Persano M, Migliari M, Pretta A, Liscia N, Astara G and Scartozzi M. Immune checkpoint inhibitors in the treatment of HCC. Front Oncol 2021; 10: 601240.
[25] Shampain KL, Hackett CE, Towfighi S, Aslam A, Masch WR, Harris AC, Chang SD, Khanna K, Mendiratta V, Gabr AM, Owen D and Mendiratta-Lala M. SBRT for HCC: overview of technique and treatment response assessment. Abdom Radiol (NY) 2021; 46: 3615-3624.
[26] Wang J, Li J, Tang G, Tian Y, Su S and Li Y. Clinical outcomes and influencing factors of PD-1/PD-L1 in hepatocellular carcinoma. Oncol Lett 2021; 21: 279.
[27] Zheng X, Liu X, Lei Y, Wang G and Liu M. Glypican-3: a novel and promising target for the treatment of hepatocellular carcinoma. Front Oncol 2022; 12: 824208.
[28] Adeva-Andany M, López-Ojén M, Funcasta-Calderón R, Ameneiros-Rodríguez E, Donapetry-García C, Vila-Altesor M and Rodríguez-Seijas J. Comprehensive review on lactate metabolism in human health. Mitochondrion 2014; 17: 76-100.
[29] Rabinowitz JD and Enerbäck S. Lactate: the ugly duckling of energy metabolism. Nat Metab 2020; 2: 566-571.
[30] Doherty JR and Cleveland JL. Targeting lactate metabolism for cancer therapeutics. J Clin Invest 2013; 123: 3685-3692.
[31] Chen AN, Luo Y, Yang YH, Fu JT, Geng XM, Shi JP and Yang J. Lactylation, a novel metabolic reprogramming code: current status and prospects. Front Immunol 2021; 12: 688910.
[32] Lv B, Wang Y, Ma D, Cheng W, Liu J, Yong T, Chen H and Wang C. Immunotherapy: reshape the tumor immune microenvironment. Front Immunol 2022; 13: 844142.
[33] Gajewski TF, Schreiber H and Fu YX. Innate and adaptive immune cells in the tumor microenvironment. Nat Immunol 2013; 14: 1014-1022.
[34] Kao KC, Vilbois S, Tsai CH and Ho PC. Metabolic communication in the tumour-immune microenvironment. Nat Cell Biol 2022; 24: 1574-1583.
[35] Xia L, Oyang L, Lin J, Tan S, Han Y, Wu N, Yi P, Tang L, Pan Q, Rao S, Liang J, Tang Y, Su M, Luo X, Yang Y, Shi Y, Wang H, Zhou Y and Liao Q. The cancer metabolic reprogramming and immune response. Mol Cancer 2021; 20: 28.
[36] Ozga AJ, Chow MT and Luster AD. Chemokines and the immune response to cancer. Immunity 2021; 54: 859-874.
[37] Oláhová M, Peter B, Szilagyi Z, Diaz-Maldonado H, Singh M, Sommerville EW, Blakely EL, Collier JJ, Hoberg E, Stránecký V, Hartmannová H, Bleyer AJ, McBride KL, Bowden SA, Korandová Z, Pecinová A, Ropers HH, Kahrizi K, Najmabadi H, Tarnopolsky MA, Brady LI, Weaver KN, Prada CE, Õunap K, Wojcik MH, Pajusalu S, Syeda SB, Pais L, Estrella EA, Bruels CC, Kunkel LM, Kang PB, Bonnen PE, Mráček T, Kmoch S, Gorman GS, Falkenberg M, Gustafs-

son CM and Taylor RW. POLRMT mutations impair mitochondrial transcription causing neurological disease. Nat Commun 2021; 12: 1135.
[38] Bonekamp NA, Peter B, Hillen HS, Felser A, Bergbrede T, Choidas A, Horn M, Unger A, Di Lucrezia R, Atanassov I, Li X, Koch U, Menninger S, Boros J, Habenberger P, Giavalisco P, Cramer P, Denzel MS, Nussbaumer P, Klebl B, Falkenberg M, Gustafsson CM and Larsson NG. Small-molecule inhibitors of human mitochondrial DNA transcription. Nature 2020; 588: 712-716.
[39] Wang Y, Ou L, Li X, Zheng T, Zhu WP, Li P, Wu L and Zhao T. The mitochondrial RNA polymerase POLRMT promotes skin squamous cell carcinoma cell growth. Cell Death Discov 2022; 8: 347.
[40] Velasco-Ruiz A, Nuñez-Torres R, Pita G, Wildiers H, Lambrechts D, Hatse S, Delombaerde D, Van Brussel T, Alonso MR, Alvarez N, Herraez B, Vulsteke C, Zamora P, Lopez-Fernandez T and Gonzalez-Neira A. POLRMT as a novel susceptibility gene for cardiotoxicity in epirubicin treatment of breast cancer patients. Pharmaceutics 2021; 13: 1942.
[41] Huang Y, Qian Y, Xing Y, Pei Y, Zhang B, Li T, Pan X, Zhong A, Du J, Zhou T and Shi M. POLRMT over-expression is linked to WNT/beta-catenin signaling, immune infiltration, and unfavorable outcomes in lung adenocarcinoma patients. Cancer Med 2023; 12: 15691-15703.
[42] Bralha FN, Liyanage SU, Hurren R, Wang X, Son MH, Fung TA, Chingcuanco FB, Tung AY, Andreazza AC, Psarianos P, Schimmer AD, Salmena L and Laposa RR. Targeting mitochondrial RNA polymerase in acute myeloid leukemia. Oncotarget 2015; 6: 37216-37228.
[43] Hayat R, Manzoor M and Hussain A. Wnt signaling pathway: a comprehensive review. Cell Biol Int 2022; 46: 863-877.
[44] Zhang Y and Wang X. Targeting the Wnt/β-catenin signaling pathway in cancer. J Hematol Oncol 2020; 13: 165.
[45] Nusse R and Clevers H. Wnt/β-Catenin signaling, disease, and emerging therapeutic modalities. Cell 2017; 169: 985-999.
[46] Xu X, Zhang M, Xu F and Jiang S. Wnt signaling in breast cancer: biological mechanisms, challenges and opportunities. Mol Cancer 2020; 19: 165.
[47] Duchartre Y, Kim YM and Kahn M. The Wnt signaling pathway in cancer. Crit Rev Oncol Hematol 2016; 99: 141-149.
[48] Taciak B, Pruszynska I, Kiraga L, Bialasek M and Krol M. Wnt signaling pathway in development and cancer. J Physiol Pharmacol 2018; 69.

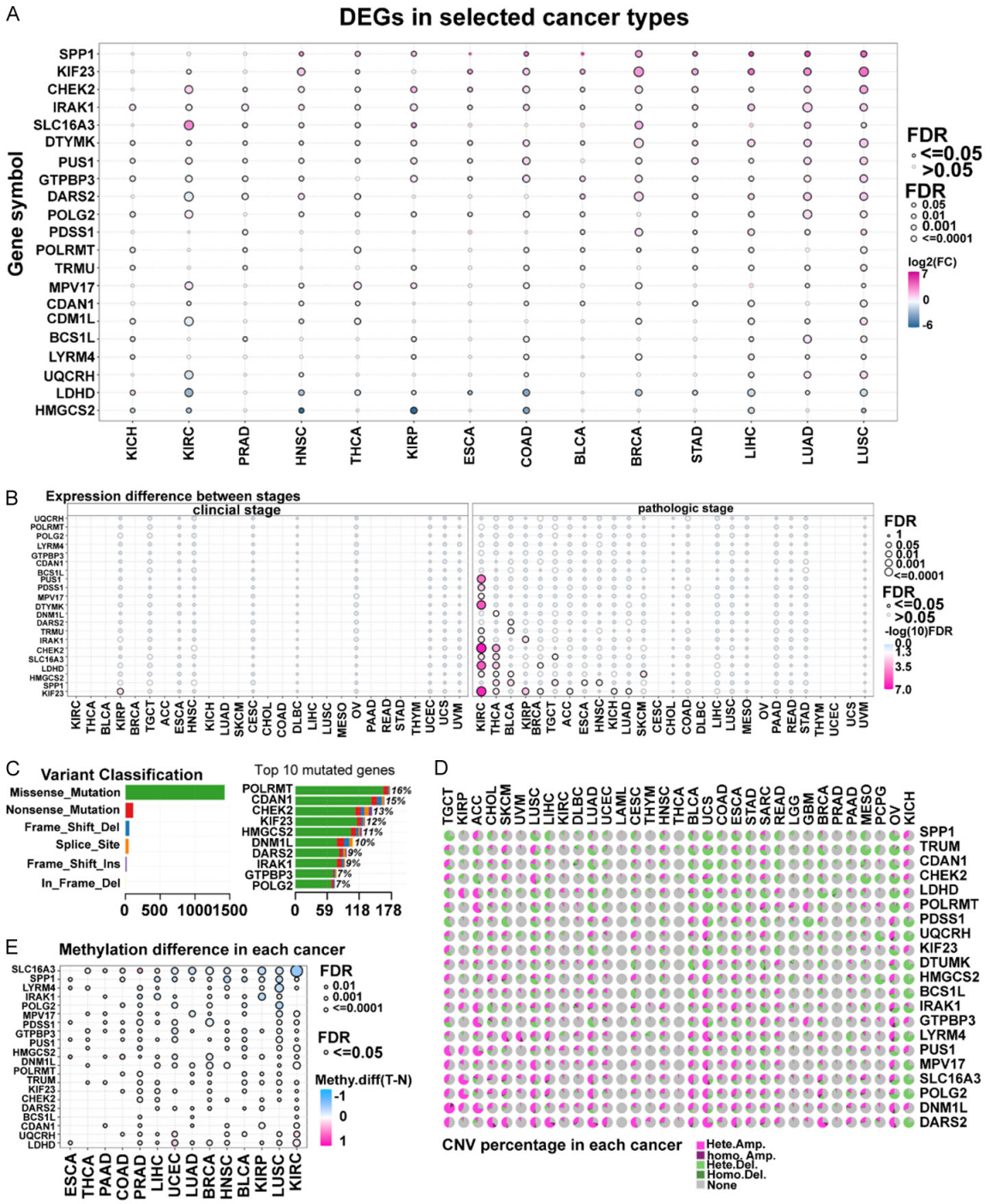

Supplementary Figure 1. The expression, genetic variants, and methylation analyses of DEGs across cancer types. A. DEGs mRNA expression across cancers. The relevance of the FDR increases with increasing dot size. The bubble's color indicates the fold change between tumor and normal tissue. B. The clinical stages and pathological stages of DEGs in cancers. C. SNV analysis including variant classification and the top 10 mutated genes in pan-cancers. D. CNV percentage of DEGs in pan-cancers. E. Methylation difference of DEGs in pan-cancers.

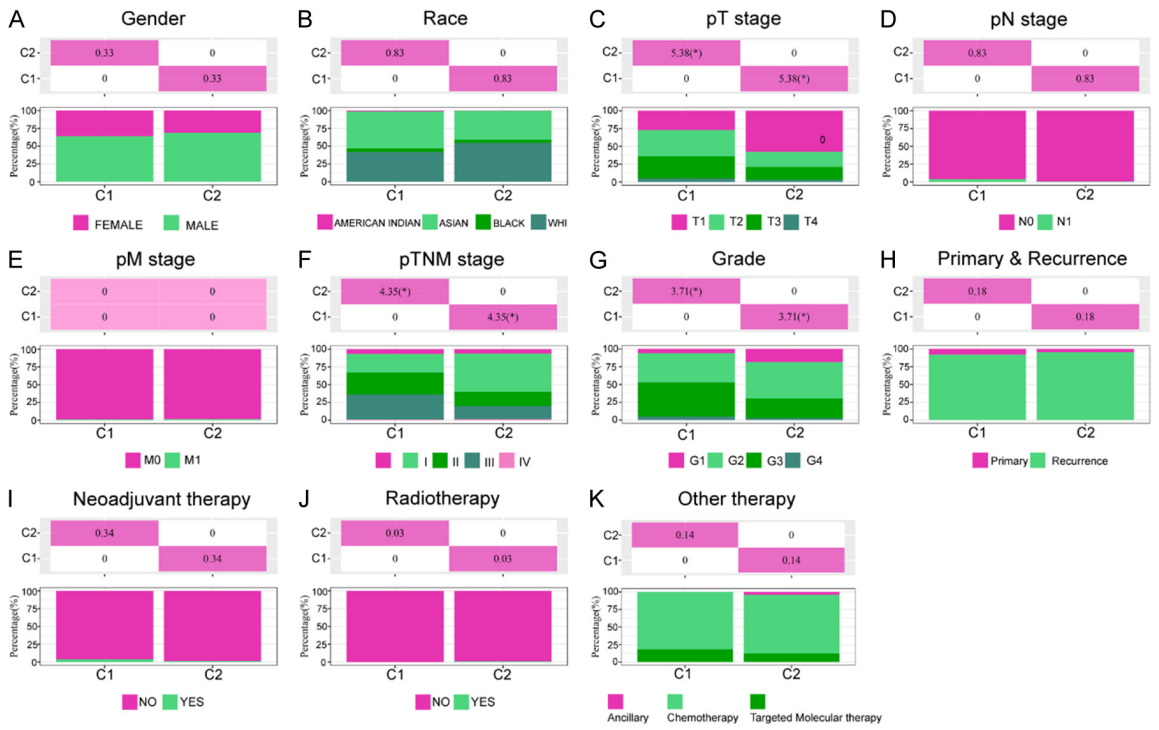

Supplementary Figure 2. The analysis of clinical information' difference in the two HCC molecular subtypes based on TCGA data. A. Gender. B. Race. C. pT stage. D. pN stage. E. pM stage. F. pTNM stage. G. Grade. H. Primary & Recurrence. I. Neoadjuvant therapy. J. Radiotherapy. K. Other therapy. C1 group: 103 HCC samples; C2 group: 268 HCC samples.

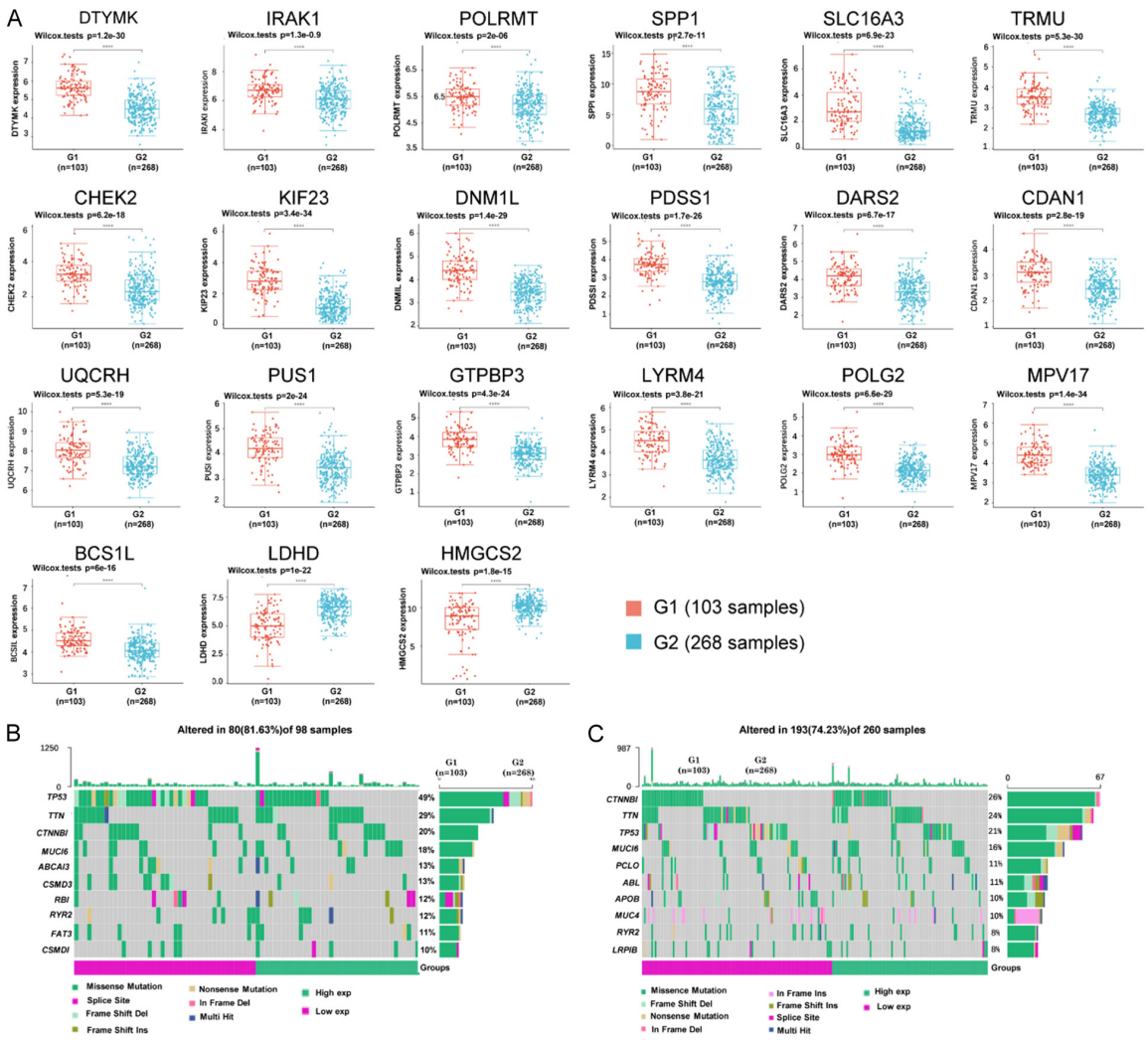

Supplementary Figure 3. The expression and genetic changes of the 21 overlap DEGs in the two HCC molecular subtypes. A. The expression of the 21 overlap DEGs in the two HCC molecular subtypes. The plots were generated by using R software. G1 group: 103 HCC samples; G2 group: 268 HCC samples. B. The waterfall plot displayed the genetic changes in group 1 subgroup (103 HCC samples). C. The waterfall plot displayed the genetic changes in group 1 subgroup (268 HCC samples).

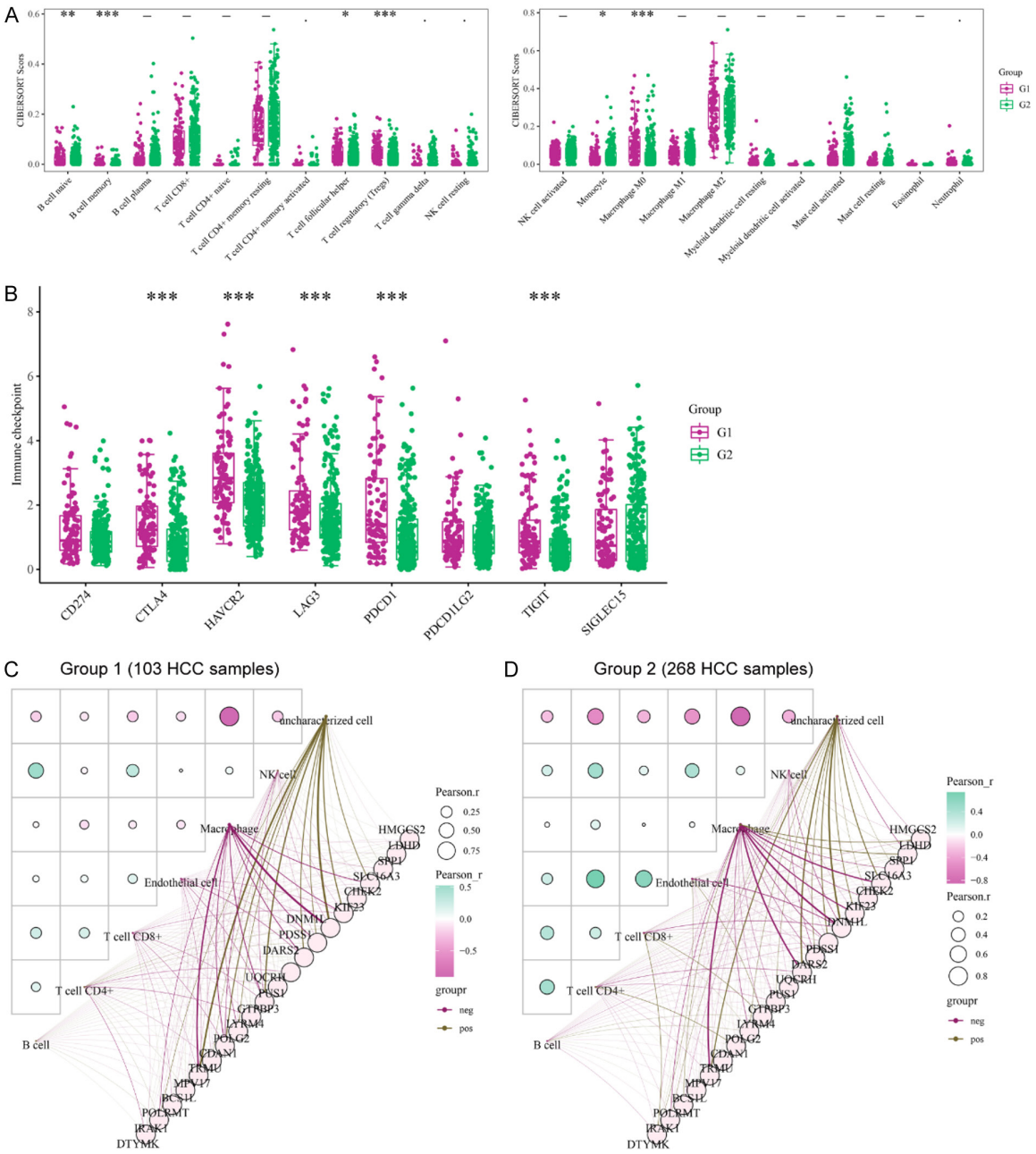

Supplementary Figure 4. Immune analysis and networks construction of the DEGs in the two HCC molecular subtypes. A. CIBERSORT score evaluated the difference of various immune cells between the two subgroups. B. The expression of the immune checkpoints in the two subgroups. C, D. The immune networks of the 21 overlap DEGs in group 1 and group 2, respectively. G1 group: 103 HCC samples; G2 group: 268 HCC samples.

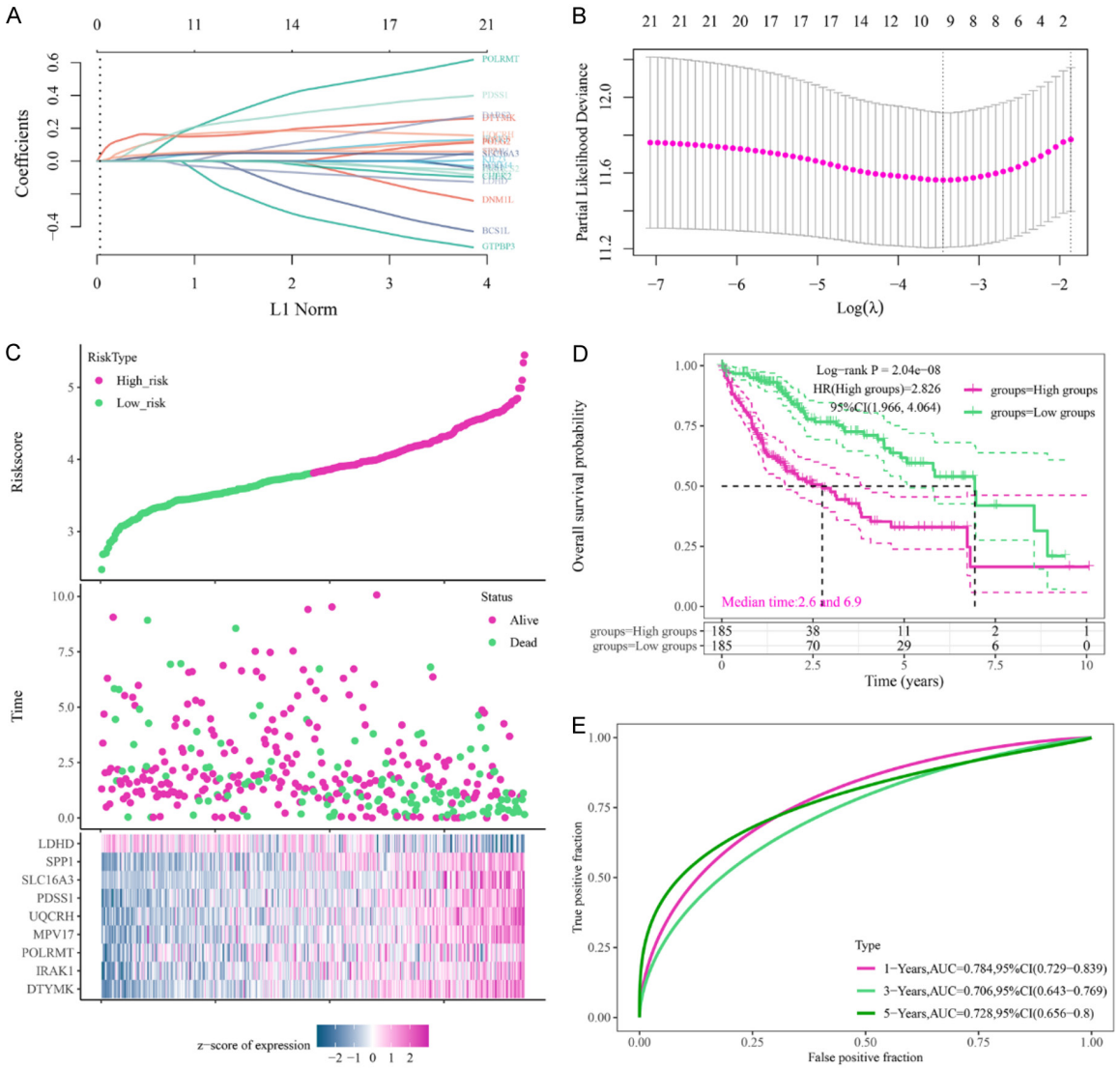

Supplementary Figure 5. Identification of 9 LRG prognostic signatures in HCC. A. LASSO coefficients profiles of 21 overlap DEGs. B. Using a ten-fold cross-validation LASSO regression, we found 9 prognostic genes with a minimal log (λ) value. C. Expression patterns of the 9 prognostic signature genes in high-risk and low-risk subgroups in HCC, together with a heatmap illustrating the relationship between risk score and survival status. D. The overall survival analysis of the high- and low-risk subgroups. E. The ROC analysis of the 9-genes prognostic signature for predicting the 1-, 3-, 5-year overall survival in HCC.

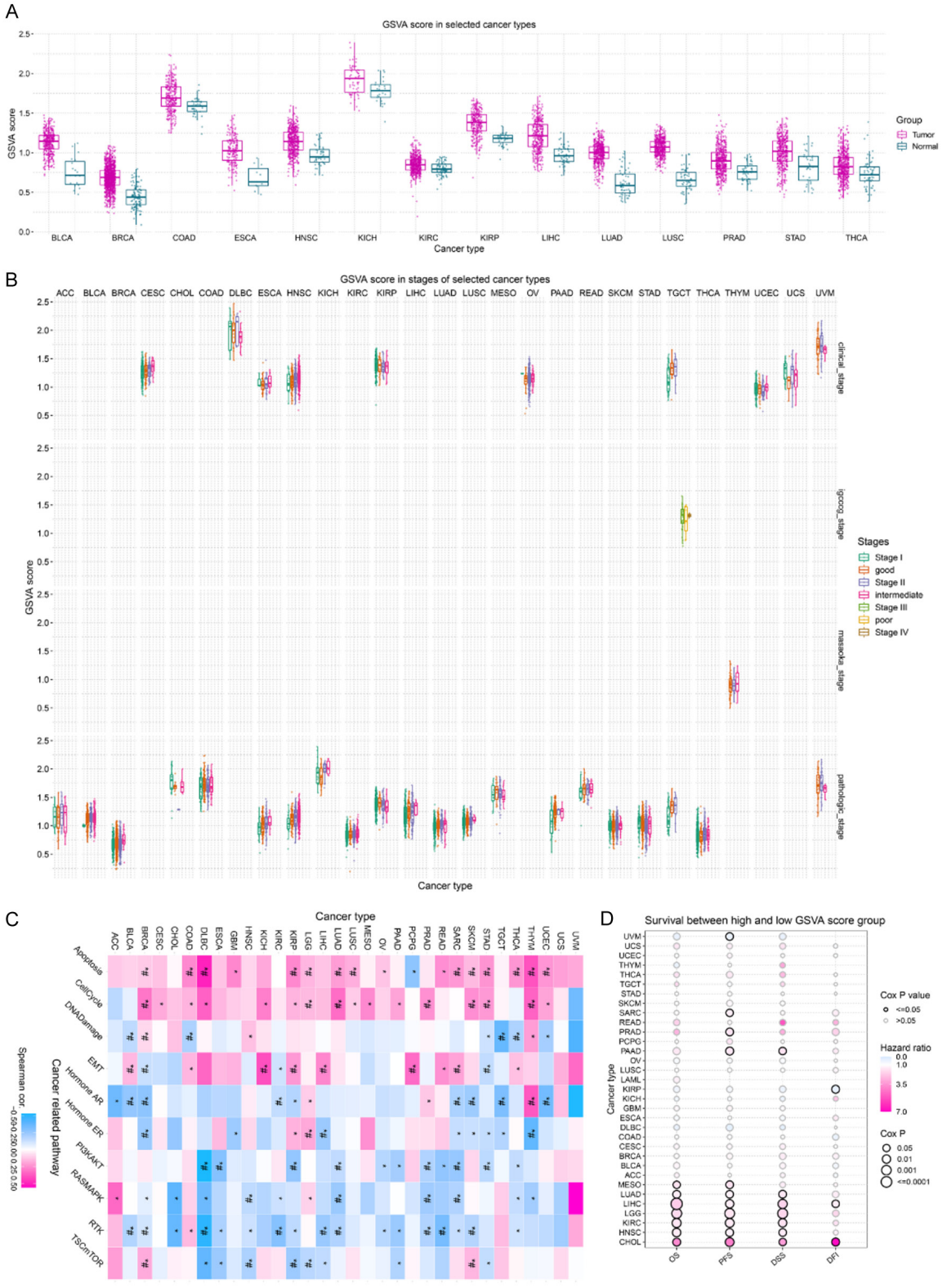

Supplementary Figure 6. GSVA analysis of the 9 prognostic signature genes in pan-cancers. A. GSVA score between tumor samples and normal tissues across cancers. The plot was generated by using GSCA database. B. GSVA score among different stages in pan-cancers. C. The correlation of the GSVA score and various pathway activities. D. The survival difference between high and low GSVA score in pan-cancers.

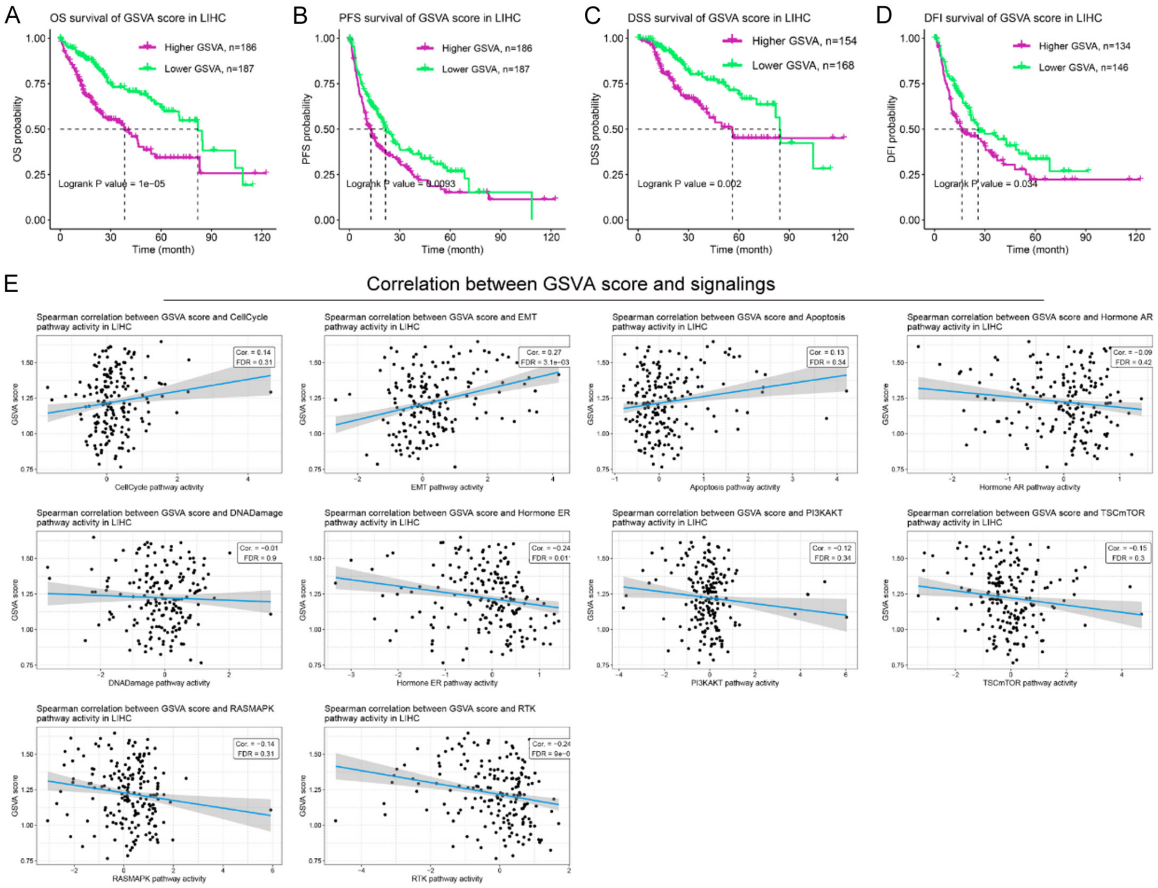

Supplementary Figure 7. GSVA analysis of the 9 prognostic signature genes in HCC. A-D. The survival difference between high and low GSVA score in HCC. E. The correlation between GSVA score and various signalings in HCC.

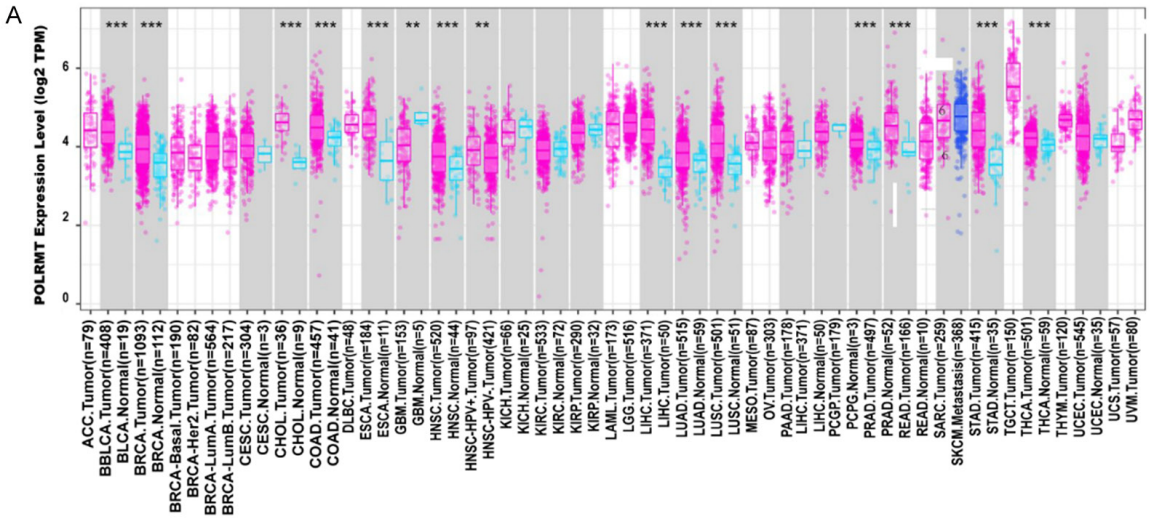
A
POLRMT Expression Level (log2 TPM)
ACC.Tumor(n=79)
BBLCA.Tumor(n=408)
BLCA.Normal(n=19)
BRCA.Tumor(n=1093)
BRCA.Normal(n=112)
BRCA-Basal.Tumor(n=190)
BRCA-Her2.Tumor(n=82)
BRCA-LumA.Tumor(n=564)
BRCA-LumB.Tumor(n=217)
CESC.Tumor(n=304)
CESC.Normal(n=3)
CHOL.Tumor(n=36)
CHOL.Normal(n=9)
COAD.Tumor(n=457)
COAD.Normal(n=41)
DLBC.Tumor(n=48)
ESCA.Tumor(n=184)
ESCA.Normal(n=11)
GBM.Tumor(n=153)
GBM.Normal(n=5)
HNSC.Tumor(n=520)
HNSC.Normal(n=44)
HNSC-HPV+.Tumor(n=97)
HNSC-HPV-.Tumor(n=421)
KICH.Tumor(n=66)
KICH.Normal(n=25)
KIRC.Tumor(n=533)
KIRC.Normal(n=72)
KIRP.Tumor(n=290)
KIRP.Normal(n=32)
LAML.Tumor(n=173)
LGG.Tumor(n=516)
LIHC.Tumor(n=371)
LIHC.Tumor(n=50)
LUAD.Tumor(n=515)
LUAD.Normal(n=59)
LUSC.Tumor(n=501)
LUSC.Normal(n=51)
MESO.Tumor(n=87)
OV.Tumor(n=303)
PAAD.Tumor(n=178)
LIHC.Tumor(n=371)
LIHC.Normal(n=50)
PCGP.Tumor(n=179)
PCPG.Normal(n=3)
PRAD.Tumor(n=497)
PRAD.Normal(n=52)
READ.Tumor(n=166)
READ.Normal(n=10)
SARC.Tumor(n=259)
SKCM.Metastasis(n=368)
STAD.Tumor(n=415)
STAD.Normal(n=35)
TGCT.Tumor(n=150)
THCA.Tumor(n=501)
THCA.Normal(n=59)
THYM.Tumor(n=120)
UCEC.Tumor(n=545)
UCEC.Normal(n=35)
UCS.Tumor(n=57)
UVM.Tumor(n=80)

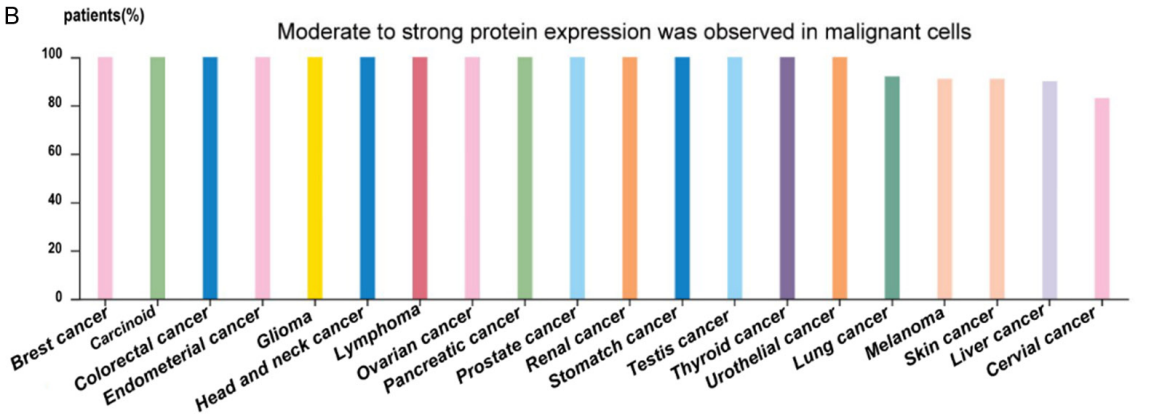
B
patients(%)
Moderate to strong protein expression was observed in malignant cells
Brest cancer
Carcinoid
Colorectal cancer
Endometerial cancer
Glioma
Head and neck cancer
Lymphoma
Ovarian cancer
Pancreatic cancer
Prostate cancer
Renal cancer
Stomatch cancer
Testis cancer
Thyroid cancer
Urothelial cancer
Lung cancer
Melanoma
Skin cancer
Liver cancer
Cervial cancer

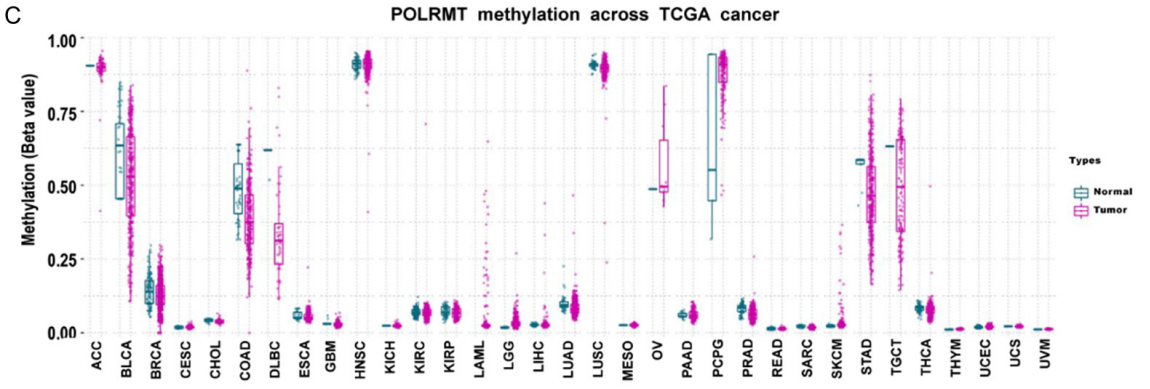
C
POLRMT methylation across TCGA cancer
Methylation (Beta value)
Types
Normal
Tumor
ACC
BLCA
BRCA
CESC
CHOL
COAD
DLBC
ESCA
GBM
HNSC
KICH
KIRC
KIRP
LAML
LGG
LIHC
LUAD
LUSC
MESO
OV
PAAD
PCPG
PRAD
READ
SARC
SKCM
STAD
TGCT
THCA
THYM
UCEC
UCS
UVM

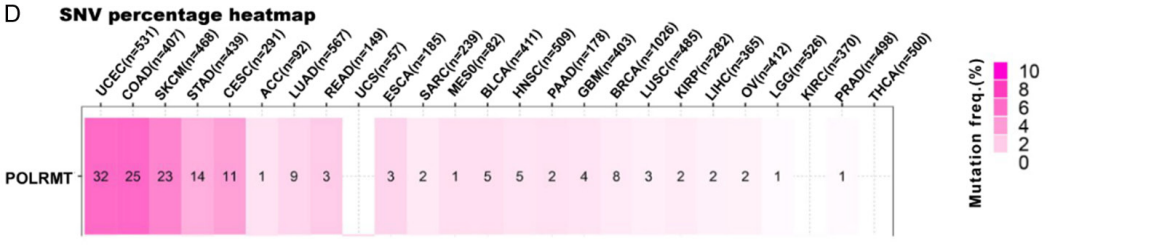
D
SNV percentage heatmap
POLRMT
32 25 23 14 11 1 9 3 3 2 1 5 5 2 4 8 3 2 2 2 1 1
Mutation freq.(%)

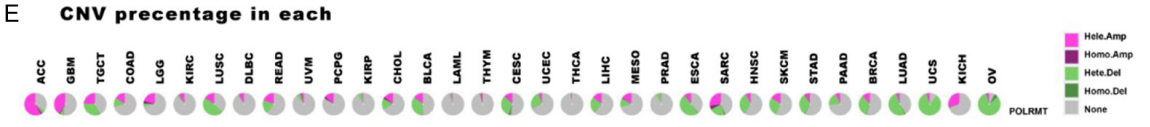
E
CNV precentage in each
Hele.Amp
Homo.Amp
Hete.Del
Homo.Del
None
POLRMT

Supplementary Figure 8. The expression, genetic changes and methylation analysis of POLRMT in pan-cancers. A. The mRNA expression of POLRMT in pan-cancers. B. POLRMT protein expression in various cancer types. C. POLRMT methylation between tumor and normal tissues across cancers. D. SNV analysis. E. CNV analysis.

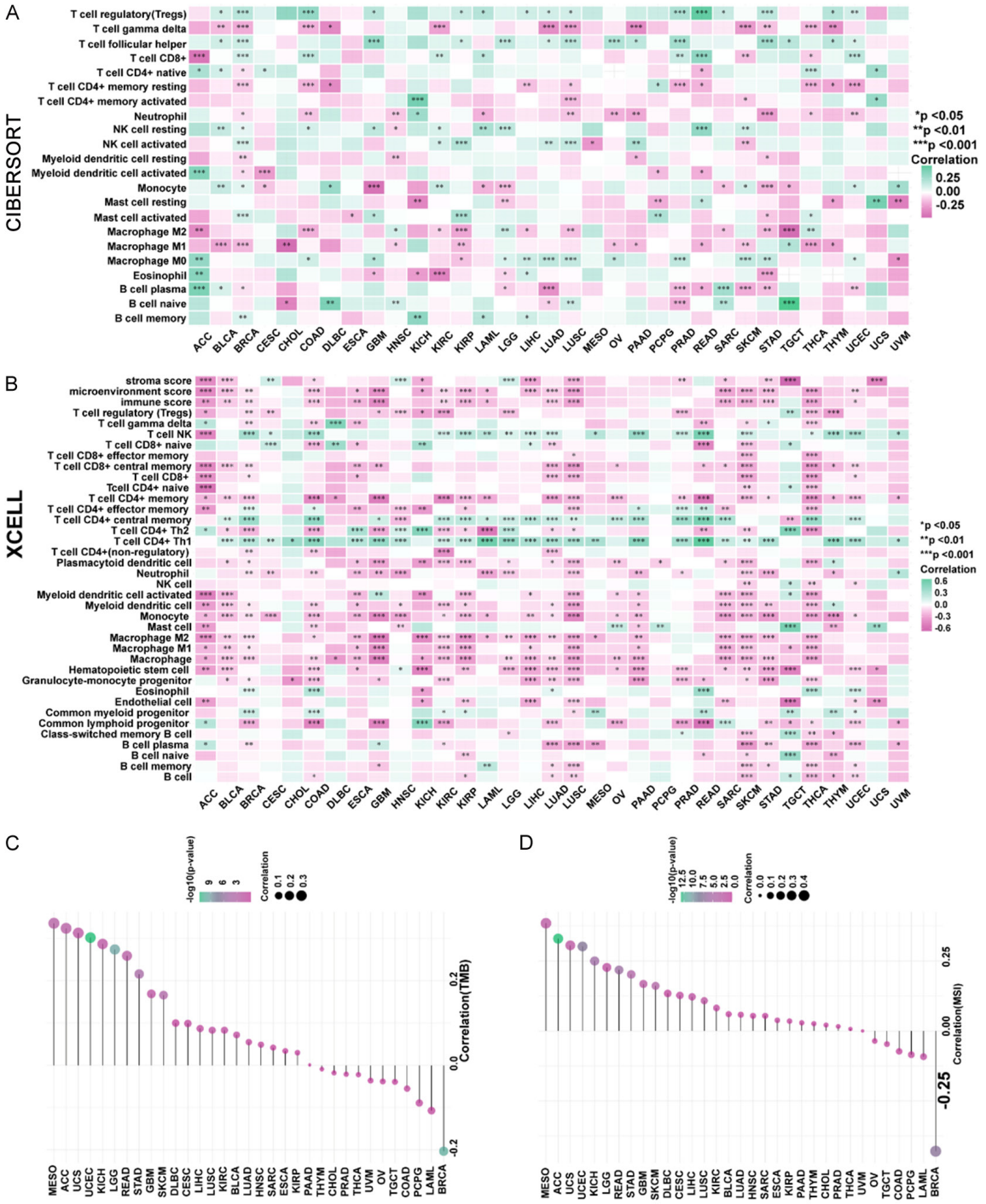

Supplementary Figure 9. Immune infiltration, TMB and MSI analyses of POLRMT in cancers. A. The immune infiltration was analyzed by CIBERSORT algorithm. B. The immune infiltration was analyzed by XCELL algorithm. C. Spearman correlation analysis of TMB and POLRMT gene expression. D. Spearman correlation analysis of MSI and POLRMT gene expression.

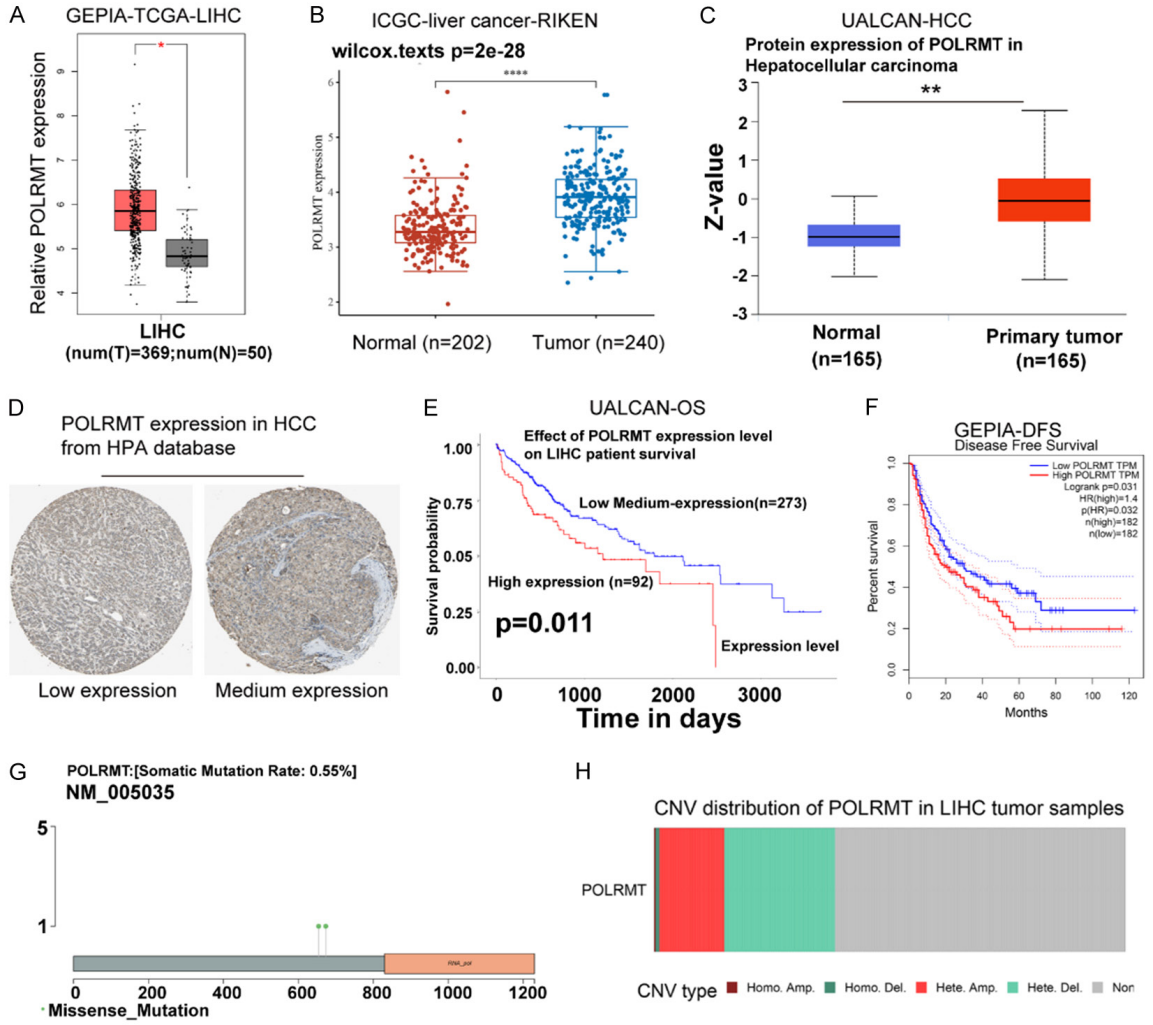

Supplementary Figure 10. The analysis of expression, survival and genetic changes of POLRMT in HCC. A. Relative POLRMT mRNA expression in tumor and normal samples using GEPIA database. B. POLRMT mRNA expression based on ICGC-liver cancer-RIKEN sub-database. C. POLRMT protein expression between normal and tumor tissues based on UALCAN database. D. The immunohistochemistry analysis of POLRMT expression based on HPA database. E. Overall survival analysis using UALCAN database. F. Disease free survival analysis using GEPIA database. G. Mutation analysis of POLRMT using GSCA database. H. CNV analysis of POLRMT using GSCA database.

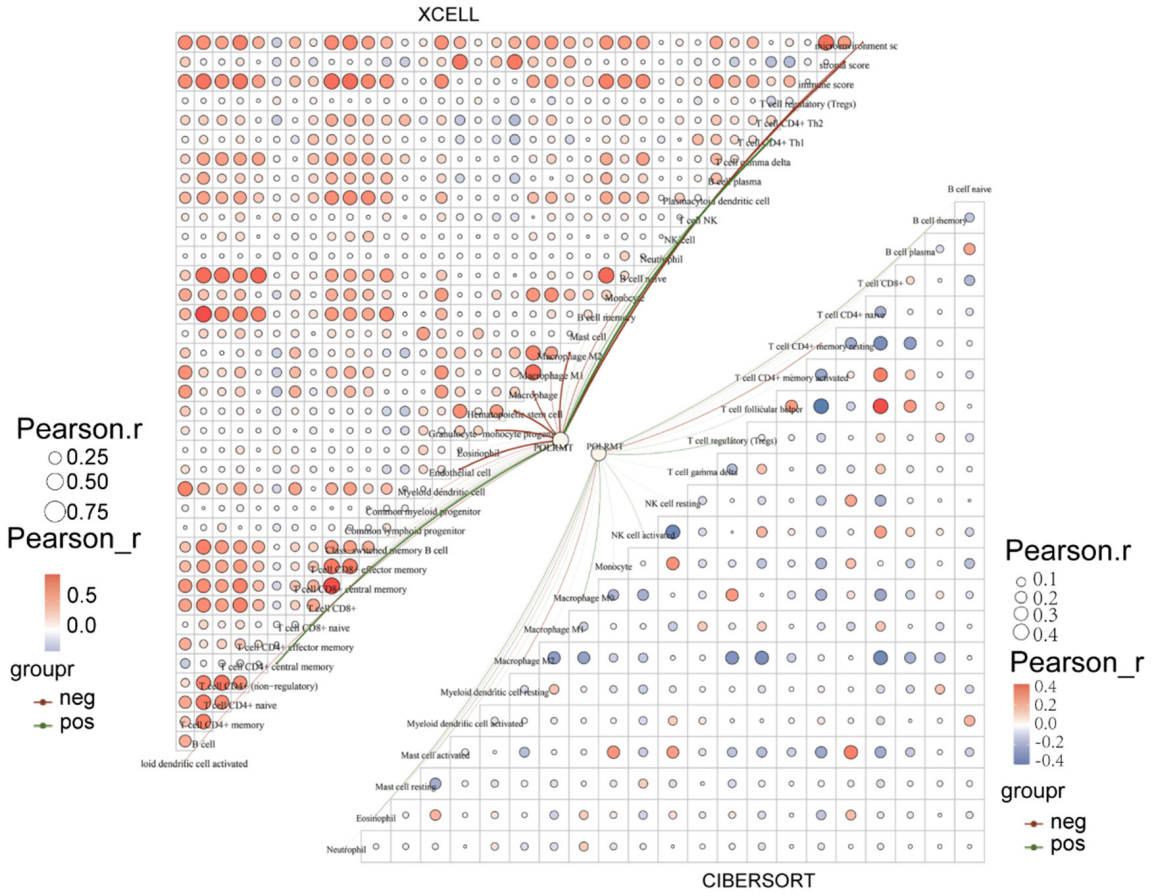

Supplementary Figure 11. The construction of the immune networks of POLRMT in HCC using XCELL and CIBERSORT algorithms. The red bubble represents positive correlation, blue bubble represents negative correlation. However, the red line represents positive correlation, blue line represents negative correlation. The more red or blue color means the greater correlation, also the larger circle means the stronger correlation.

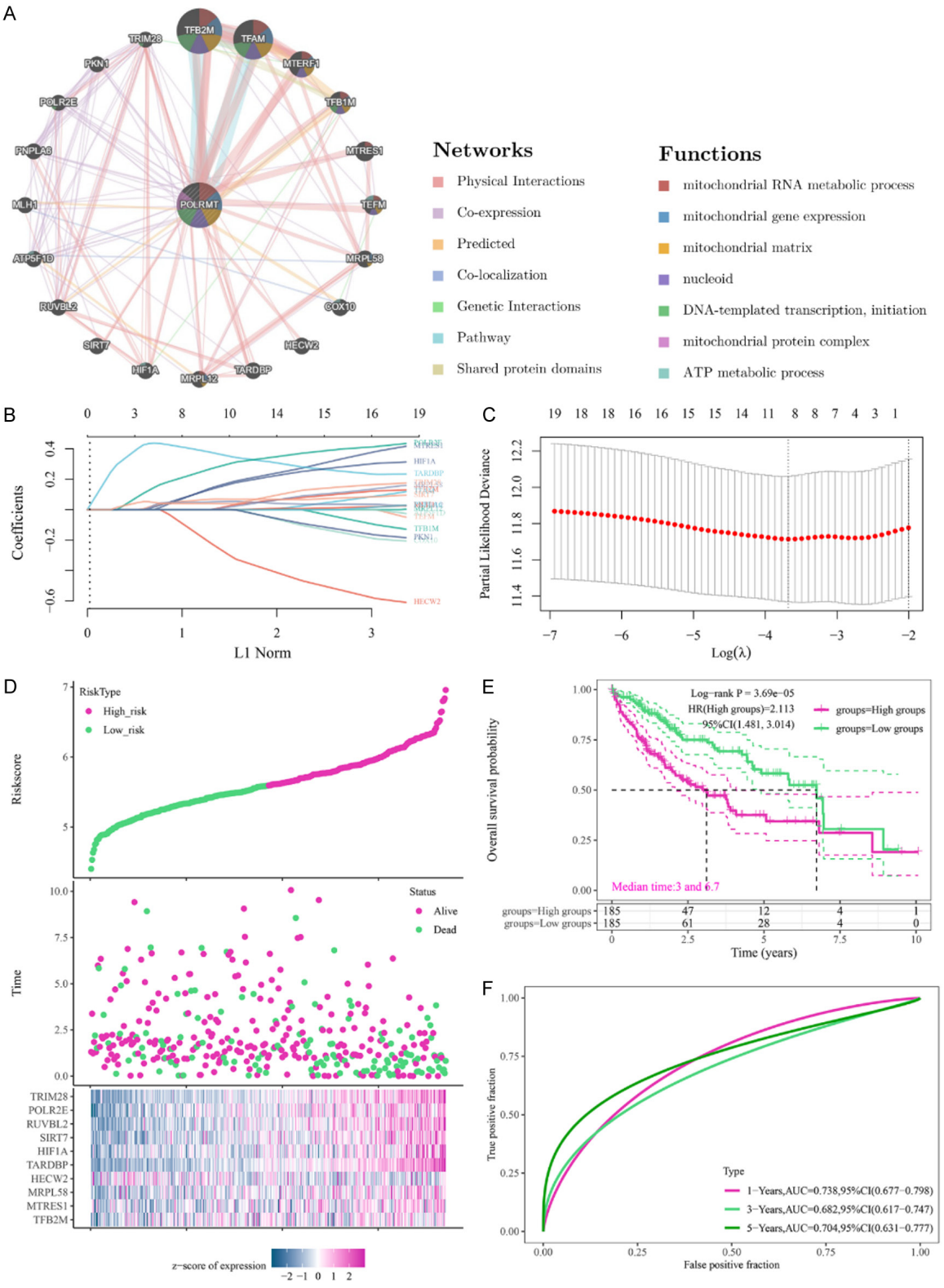

Supplementary Figure 12. POLRMT interacting network and prognostic signature construction based on its interacting genes. A. The interacting network of POLRMT was generated by using GeneMania database. B. LASSO coefficients profiles of 20 POLRMT interacting genes. C. LASSO regression with tenfold cross-validation obtained 10 prognostic genes using minimum log (λ) value. D. Expression patterns of the 10 prognostic signature genes in high-risk and low-risk subgroups in HCC, together with a heatmap depicting the relationship between risk score and survival status. E. The overall survival analysis of the high- and low-risk subgroups. F. Predicting 1-, 3-, and 5-year overall survival in HCC using a signature of 10 genes: ROC analysis.

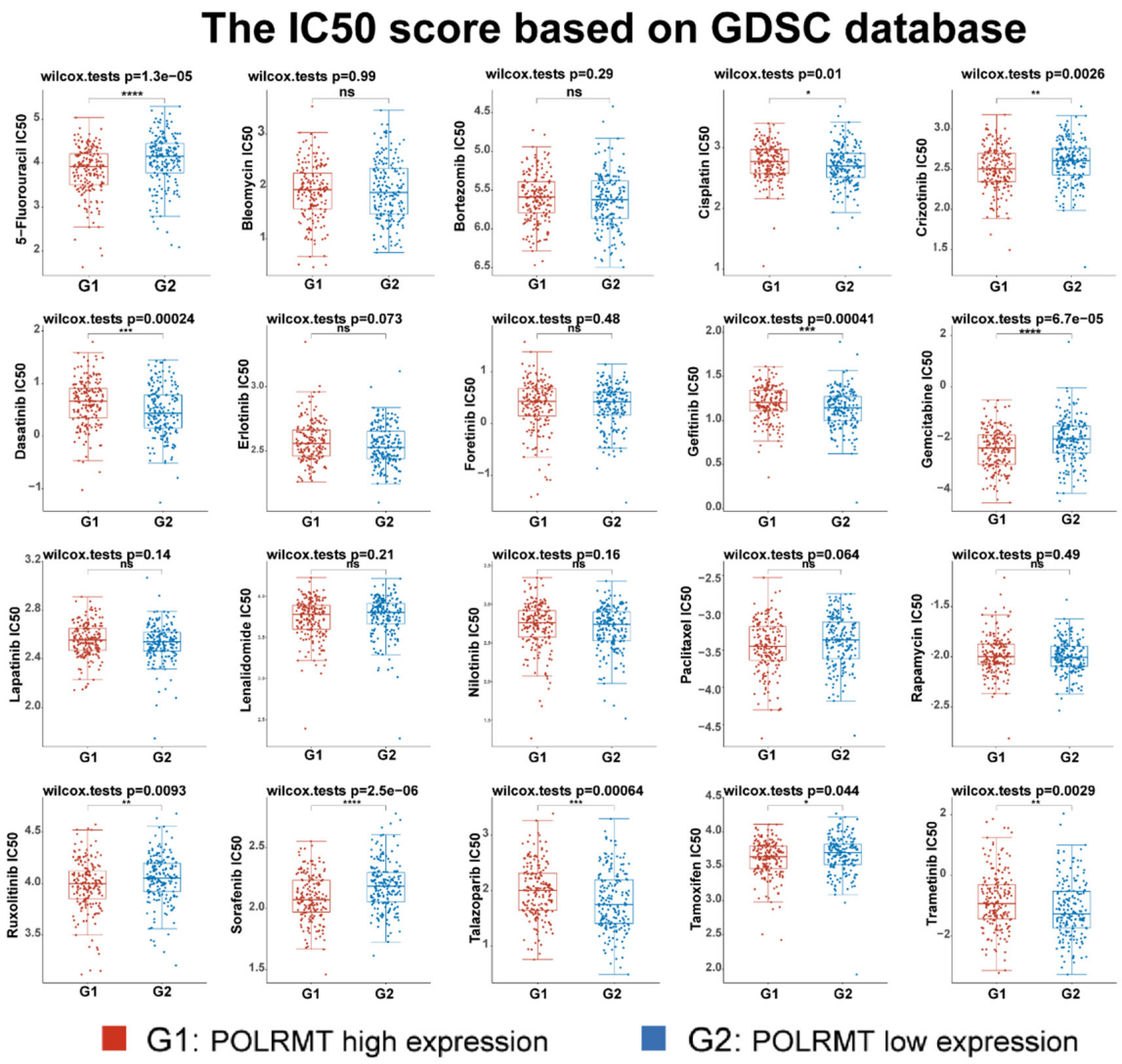

Supplementary Figure 13. IC50 scores analysis of drugs targeting HCC in POLRMT high and low expression groups.